2024

Contamination Assessment and Reduction Project – Phase 2 (CARP II)

Appendix A-3. Sediment Bioaccumulation Estimates and Prediction of HARS Suitability

Objective 4: Refine method for predicting bioaccumulation of sedimentary contaminants in dredged material test organisms

NY/NJ Harbor Contamination Assessment and Reduction Project

CARP II

Develop a method (or model) for predicting bioaccumulation of sedimentary contaminants in dredged material test organisms

New Jersey Department of Transportation,

Under Agreement with Monmouth University and the Hudson River Foundation

July 2023

Kevin J. Farley[1], Nelson da Luz[1,2], Jacqueline DeLorenzo[1,3], Ellen Farrelly[1,4], Robin E. Landeck Miller[5], James Lodge[6], Rainer Lohmann[7], Simon Vojta[7]

[1]Manhattan College, Riverdale NY, [2]currently at The University of Massachusetts, Amherst MA, [3]currently at Gannett Fleming Engineers and Architects, New York NY, [4]currently at Geosyntec Consultants, Lyndhurst NJ, [5]1HDR Inc., Woodcliff Lake NJ, [6]Hudson River Foundation, New York NY, [7]Univeristy of Rhode Island, Narragansett RI.

Introduction

The overall goals of the Contamination Assessment and Reduction Project II (CARP II) were to: (i) evaluate current and future contamination of New York-New Jersey (NY-NJ) Harbor sediments, and (ii) determine if and when dredged material from the harbor would meet criteria for disposal at the Historic Area Remediation Site (HARS). For current assessments, HARS suitability is based on 28-day bioaccumulation tests using the dredged material test organism *Neanthes virens* (formerly classified as *Nereis virens*). Although the 28-day bioaccumulation tests provide a justifiable method for assessing HARS suitability, bioaccumulation testing can be costly, and more importantly, test results are of limited value in evaluating HARS suitability for future projections of sediment contamination. Therefore, the primary purpose of this task was to develop a quantitative method for linking current and future projections of sediment contamination to contaminant accumulation in the dredged material test organism, *N. virens*.

Specific contaminants of concern in these studies are polychlorinated biphenyls (PCBs) and 2,3,7,8-substituted polychlorinated dibenzo-p-dioxins and dibenzo-furans (PCDD/Fs). Previous studies on PCB and PCDD/F accumulation in test organisms (including *N. virens* and *Lumbriculus variegatus*) have utilized Biota Sediment Accumulation Factors (BSAFs) to relate contaminant concentrations in sediments to contaminant accumulation in the organisms. Large variations in BSAFs however have been reported for 28-day bioaccumulation tests for NY-NJ Harbor (Farley et al. 1999, HydroQual 2007) and at other sites throughout the United States (McLeod et al. 2007, Burkhard et al. 2013). Similar findings were also reported for BSAFs from field-collected samples in the original NY-NJ Harbor CARP study (HydroQual 2007; Miller et al. 2011).

The presence of multiple binding phases in sediments (including soot or black carbon) has been cited as a possible reason for large variations in contaminant bioavailability and associated BSAF values (Lohmann et al. 2005; Friedman et al. 2009). These evaluations of bioavailability in sediments have largely been based on results from polyethylene samplers (to measure porewater concentrations) and thermochemical oxidation of sediments (to estimate black carbon content). In addition to bioavailability, other factors such as the nutritional content of the sediment organic carbon, organism bioenergetics and feeding behavior may play a role in ultimately determining PCB and PCDD/F bioaccumulation behavior.

The primary objectives of this task were therefore defined as follows:

1. Evaluate the current bioaccumulation potential of harbor sediments using CARP II 28-day bioaccumulation test results for the dredged material test organism *N. virens*.

2. Determine BSAFs that can be used in evaluating PCB and PCDD/F accumulation in *N. virens* based on model projections for future sediment contamination levels.

3. Evaluate the effects of sediment (f_{TOC}, f_{Soot}), organism (f_{Lipid}) and chemical (log K_{ow}, chemical structure) properties on BSAFs.

4. Examine sediment-water partitioning (K_p's) and organism-water partitioning (BAFs) using the 20 sediment samples with measured porewater concentrations.

5. Develop K_p, BAF and BSAF relationships for PCB congeners as a function of sediment (f_{TOC}, f_{Soot}), organism (f_{Lipid}) and chemical (log K_{ow}, chemical structure) properties, and test the applicability of the PCB relationships to PCDD/F congeners.

Methods

Field sampling: Sediment samples were collected from six locations in NY-NJ Harbor: Buttermilk Channel, Elizabeth Channel, Port Jersey, Port Newark Channel, South Brother Island Channel and Ward Point Bend near the mouth of the Raritan River. At each location, three samples were collected in the navigation channel and three samples were collected from off-channel sediments. One exception was Port Newark Channel where only one sample was collected from the off-channel sediments. A full list of sample locations is provided in Table A-1 in the appendix.

Sediment samples were collected using a KC HAPS bottom corer. Navigation channel core samples were sub-sampled with a 0-10 cm sediment sample to represent recently deposited material and typically a 20-30 cm sample to represent older sediments that are typically considered in dredged material testing. Since off-channel sediments are expected to accumulate at slower rates, sediment samples were sub-sampled with a 0-4 cm sediment sample to represent recently deposited material and typically a 6-10 cm sample to represent older sediments. See Table A-1 for a full list of sediment core sub-sampling depths.

In all, a total of 68 sediment samples were collected from in-channel and off-channel areas throughout the harbor. As described below, sediment samples were forwarded to various laboratories for sediment chemical analyses and 28-day bioaccumulation testing.

Sediment chemical analyses: Each of the 68 sediment samples were analyzed by SGS AXYS for PCB congeners (using SGS AXYS Method MLA-010 Rev 12) and 2,3,7,8-substituted PCDD/Fs (using SGS AXYS Method MLA-017 Rev 20). Additional sediment analyses were performed by Alpha Analytical for total organic carbon (Alpha Analytical Method 9060A) and soot content (Alpha Analytical Method 9060, modified, phosphoric acid instead of HCl). Dissolved organic carbon concentrations in sediment porewater were also determined by SGS Accutest New Jersey (Method SM5310 B-11). Berylium-7 measurements were performed by Pace Analytical (EPA Method 901.1). Finally, a subset of 20 sediment samples were forwarded to R. Lohmann, University of Rhode Island (URI) for supplemental chemical analyses. These included PCB and PCDD/F porewater concentrations using polyethylene passive samplers and black carbon content of sediments based on a thermal oxidation method (see Lambert et al. 2011 for details).

28-day bioaccumulation testing: 28-day bioaccumulation tests were performed by EcoAnalysts, Inc. using criteria outlined in the US Army Corps of Engineers – New York District (USACE-NYD) and the United States Environmental Protection Agency (USEPA) Region 2 Testing Manual (USACE/USEPA 2016). Briefly, test worms (*N. virens*) were obtained from Aquatic Research Organisms Inc. in Hampton, New Hampshire and

held at 20±2°C prior to testing. Testing was performed in 9.5 L (2.5-gallon) aquaria which were modified with overflow standpipe water ports. Each test chamber was loaded with approximately 2 L of sediment to a depth of 5 cm and was filled with approximately 5.3 L of overlying water. During exposures, test chambers were aerated and a continuous supply of seawater was provided to maintain approximately six water exchanges per day.

Bioaccumulation tests were conducted in two batches. Batch #1 included sediment samples from Buttermilk Channel, South Brother Island Channel, Ward Point Bend that were collected between 26 March 2019 and 23 April 2019. Batch #2 included sediment samples from Elizabeth Channel, Port Jersey, Port Newark Channel that were collected between 7 May 2019 and 13 June 2019. For each batch, tests were conducted on three control replicates (with sediments from the Damariscotta River, Boothbay Harbor, Maine as provided by Aquatic Research Organisms) and on single replicates for each of the NY-NJ Harbor sediment samples.

Bioaccumulation tests were initiated by adding eight worms to each chamber. Salinity, pH, temperature, and dissolved oxygen were monitored daily. On Day 28, sediments were sieved to recover the worms and the surviving animals were placed in clean flow-through aquaria in the absence of sediment for 24 hours to allow purging of their gut contents. The worms were then rinsed with deionized water, placed in certified pre-cleaned glass containers and frozen. Tissues from all sediment exposures (with the exception of the laboratory controls) were delivered via overnight courier to SGS AXYS (Sidney, British Columbia, Canada) for chemical analyses.

Data analyses: Data used in bioaccumulation evaluations were extracted from the CARP II Microsoft Access database (give reference) and analyzed in Microsoft Excel. A full description of Microsoft Access data queries and organization of data in the Excel worksheets is provided in Appendix B.

Subsequent evaluations of the data are outlined below:

For the first objective, 28-day bioaccumulation test results of tissue concentrations were compiled for total PCBs, 2,3,7,8-TCDD and total Toxic Equivalents (TEQs). Following EPA Region 2 protocols for total PCB evaluations, PCB tissue concentrations from the 28-day bioaccumulation tests were multiplied by a factor of two to convert 28-day accumulations to steady-state estimates (Landeck Miller et al. 2023). For 2,3,7,7-TCDD and total TEQ evaluations, concentrations were determined directly from 28-day bioaccumulation test results using measured tissue concentrations of PCDD/Fs and dioxin-like PCBs. Total TEQs were determined as:

$$Total\ TEQ = \sum TEF \times \nu_{Tissue} \quad \text{(Eq. 1)}$$

where TEF is Toxic Equivalent Factor and ν_{Tissue} is the chemical concentration in the organism in ng chemical/kg wet wt (or comparable units). Estimates for organism accumulation were then compared to dredged material bioaccumulation guidelines for HARS disposal; i.e., 113 ppb for Total PCBs, 1 ppt for 2,3,7,8-TCDD and 4.5 ppt for total TEQs.

For the second objective, BSAFs were calculated for PCB homologs and PCDD/F congeners using paired tissue wet weight and sediment dry weight concentrations from the 28-day bioaccumulation tests:

$$BSAF = \frac{\nu_{Tissue}}{r_{Sediment}} \quad \text{(Eq. 2)}$$

where ν_{Tissue} and $r_{Sediment}$ are the chemical concentration in the organism (in ng chemical/kg wet wt) and on the sediment (in ng chemical/kg dry wt), respectively. Calculated BSAFs for the 68 sediment samples were analyzed using probability plots to examine spatial variability and to determine median (50th percentile) and 90th percentile values. Median and 90th percentile values were also compared to current dredged material management guidelines for select PCB homologs and for 2,3,7,8-TCDD.

For the third objective, correlation coefficients were calculated to examine potential relationships of 28-day BSAFs to sediment properties (f_{TOC}, f_{Soot}), lipid content (f_{Lipid}) and f_{Lipid}/f_{TOC}. Lipid:organic carbon normalized BSAFs ($BSAF_{lipid,oc}$) were also computed:

$$BSAF_{lipid,oc} = \frac{\nu_{Lipid}}{r_{oc}} \quad \text{(Eq. 3)}$$

where ν_{Lipid} and r_{oc} are the chemical concentration in the organism (in ng chemical/kg lipid) and on sediments (in ng chemical/kg organic carbon), respectively. $BSAF_{lipid,oc}$ probability plots were then developed and compared to the non-normalized BSAF probability distributions to see if lipid:organic carbon normalization of BSAFs was warranted. Finally, variations in BSAFs were examined as a function of log K_{ow} values to examine the effects of chemical hydrophobicity and chemical structure on BSAFs.

For the fourth objective, sediment-water partitioning coefficients (K_p) and 28-day BioAccumulation Factors (BAFs) were examined using the 20 sediment samples with porewater measurements. For this evaluation, K_p and BAF values were calculated for PCB homologs, PCB congeners and PCDD/F congeners as:

$$K_p = \frac{r_{Sediment}}{C_{Porewater}} \quad \text{(Eq. 4)}$$

$$BAF = \frac{\nu_{Tissue}}{C_{pw}} \quad \text{(Eq. 5)}$$

where C_{pw} is the chemical concentration in porewater (in ng chemical/L) as determined in the laboratory using polyethylene samplers. K_p and BAF results were plotted as a function of the log of the octanol-water partition coefficient (log K_{ow}) to evaluate similarities and differences in PCB, PCDD and PCDF behavior.

For the fifth objective, K_p, BAF and BSAF relationships were developed for PCB congeners as a function of sediment, organism and chemical properties. For K_p evaluations, parameters included the amorphous organic carbon content ($f_{aoc} = f_{TOC} - f_{BC}$) and black carbon content (f_{BC}) of the sediment, temperature and salinity corrected log K_{ow} values [log K_{ow}(T,S)] described below and the dihedral angle of the PCB congeners. Here, the dihedral angle is the angle between the two benzene rings of the PCB molecule which is known to increase with increasing number of ortho-substituted chlorines on the biphenyl

structure. The final K_p relationship (and associated model coefficients) was determined in Microsoft EXCEL using SOLVER to minimize the sum of the squares of the 'log K_p(calculated) – log K_p(observed)' residuals. SOLVER calculations were based on the GRG (generalized reduced gradient) algorithm, a maximum of 100 iterations, a precision of 1×10^{-6}, central differencing of numerical derivative, and unconstrained variables constrained to non-negative values.

Similar calculations were performed in developing a relationship for BAF as a function of the lipid content (f_{Lipid}) of the organisms and log K_{ow} of the PCB congeners. Results from the K_p and BAF equations were then used to calculate BSAFs as:

$$BSAF(calculated) = \frac{BAF(calculated)}{K_p(calculated)} \quad \text{(Eq. 6)}$$

Calculated BSAFs were then compared to observed BSAF values. Finally, the PCB K_p, BAF and BSAF relationships were applied to PCDD/F congeners to test the applicability of the PCB-derived relationships to PCDD/Fs. For these calculations, PCDD/F congeners were considered to be planar with a dihedral angle equal to '0'.

Chemical parameters: Chemical parameters used in data analyses described above were obtained as follows: log K_{ow} values for PCB congeners were taken from Hawker and Connell (1988). For co-eluting congeners and PCB homologs, log K_{ow} values were determined from averages of the log K_{ow} congener values. Log K_{ow} values for PCDD/F congeners were taken from Sacan et al. (2005) as cited in Cornelissen et al. (2008).

Since log K_{ow} values were reported in terms of 25°C and 0 salinity, temperature and salinity corrections were made to bioaccumulation test conditions of 19°C and 30 psu. Temperature corrections were based on the van't Hoff equation:

$$logK_{ow}(T) = logK_{ow}(25°C) + \frac{\Delta H_{ow}}{2.303\times R}\left[\frac{1}{298.15} - \frac{1}{(273.15+T)}\right] \quad \text{(Eq. 7)}$$

where ΔH_{ow} is the enthalpy for the octanol-water phase change. ΔH_{ow} values for PCB congeners were computed by Greene et al. (2013) as a function of total chemical surface area (TSA):

$$\Delta H_{ow} = -0.0636 \times TSA_{cavity} - 6.09 \quad \text{(Eq. 8)}$$

The above ΔH_{ow} relationship was also used to estimate ΔH_{ow} values for PCDD/F congeners using TSA values for PCDDs (Friesen and Webster 1990) and PCDFs (Dunn III et al. 1986) as cited in Mackay et al. (1992). Salinity corrections were based on Setschenow equation:

$$logK_{ow}(S) = logK_{ow}(freshwater) + K^{salt} \cdot [salt] \quad \text{(Eq. 9)}$$

where values for K^{salt} (the Setschenow constant) were obtained from the UFZ-LSER database v 3.2.1 (Ulrich et al. 2017) and [salt] is the molar salt concentration (≈ 0.6 · salinity / 35 psu).

A complete listing of chemical parameters for PCB congeners and PCDD/F congeners is given in Tables A-2 and A-3 in the appendix. For co-eluting PCB congeners and PCB homologs, log K_{ow}, ΔH_{ow} , and K^{salt} values were determined from averages of the congener values. A listing of PCB co-eluting congeners is given in Table A-4 in the appendix. Because the AXYS and URI quantification methods for PCB congeners had slight differences, several adjustments of co-eluting PCB congener list were also required (see Table A-4 footnote).

Results and Discussion

28-day Bioaccumulation Test Results: Bioaccumulation test results for the 68 sediment samples that were collected throughout NY-NJ Harbor are presented in Figure 1 for PCBs and for 2,3,7,8-TCDD toxic equivalents. As noted previously, PCB tissue concentrations from the 28-day bioaccumulation tests were multiplied by a factor of two to convert 28-day accumulations to steady-state estimates (Figure 1a). TEQ results were determined directly from the 28-day bioaccumulation results without adjustment to steady state (Figure 1b). Current dredged material management guidelines for HARS disposal are also presented in Figure 1 for comparison to the bioaccumulation results.

As shown in Figure 1a, tetra-, penta- and hexa-CB were found to be the dominant PCB homologs that accumulated in the test organisms. Four of the 68 sediment samples exceeded the Total PCB dredged material management guideline of 113 ppb. Of particular note is that the four sediment samples that were in exceedance of the 113 ppb guideline were collected outside the navigation channel. Steady-state bioaccumulation results for sediments within the navigation channel were typically 2-3 times below the 113 ppb guideline.

Not surprisingly, the TEQ results for NY-NJ Harbor are dominated by 2,3,7,8-TCDD, followed by 1,2,3,7,8-PeCDD; 2,3,7,8-TCDF, 2,3,4,7,8-PeCDF and dioxin-like PCBs. All sediment samples from the navigation channel and off-channel areas of Port Newark Channel (PNC) exceeded the 1 ppt guideline for 2,3,7,8-TCDD. In addition, navigation channel and off-channel areas of Elizabeth Channel (EC) exceeded or were close to exceeding the 2,3,7,8-TCDD guideline (1 ppt). Only one sample (PNC-OC-1-L) from Port Newark Channel exceeded the Total TEQ guideline of 4.5 ppt.

BSAFs for PCB homologs and PCDD/F congeners: 28-day BSAF results for 68 sediment samples are presented as probability distributions for several PCB homologs and PCDD/F congeners in Figure 2. The BSAF probability distributions for all PCB homologs and PCDD/F congeners are included in Figures A-1 through A-3 in the appendix. As shown, computed BSAFs vary by roughly an order of magnitude for each of the PCB homologs and PCDD/F congeners. Computed BSAFs are also shown to be log normally distributed, as indicated by the close adherence of BSAFs to the linear trendlines on the semi-log plots. However, some exceptions to the log normal distributions are noted for the highest 4 or 5 BSAFs where observed values for the more chlorinated PCB homologs and many of the PCDD/F congeners lie above the linear trendlines.

EPA Region 2 recommended BSAF values that are currently used in dredged material evaluations are also included on Figure 2 for the PCB homologs and for 2,3,7,8-TCDD. The EPA BSAF estimates were purposely

plotted with a Z-score corresponding to the 90th percentile. A summary of probability distribution results (including slopes and intercepts of the linear trendlines, as well as median and 90th percentile 28-day BSAF values) are presented in Tables 1 and 2 for the PCB homologs and the PCDD/F congeners, respectively. As shown, the current EPA BSAF estimates are roughly an order of magnitude higher than the 90th percentile value for di-CB, approximately a factor of 2 higher than the 90th percentile value for tetra-CB, and within a factor of two of the 90th percentile values for hexa-CB, octa-CB and 2,3,7,8-TCDD.

Effects of sediment, organism and chemical properties on BSAFs: Calculated correlation coefficients for potential relationships of 28-day BSAFs to f_{TOC}, f_{Soot} and f_{Lipid} are presented for PCB homologs and PCDD/F congeners in Tables 3 and 4, respectively. As shown, BSAFs have a moderate negative correlation to f_{TOC}. Somewhat surprisingly, BSAFs were determined to have a very weak correlation to f_{Lipid} and a weak to moderate positive correlation to f_{Soot}. Correlations of BSAFs to f_{Lipid}/f_{TOC} were also computed to see if lipid:organic carbon normalization of the BSAF values was warranted. Results show that BSAFs for the PCB homologs have a moderate positive correlation to f_{Lipid}/f_{TOC} and BSAFs for the PCDD/F congeners have a weak to moderate correlation to f_{Lipid}/f_{TOC}.

Based on correlation results in Tables 3 and 4, we would not expect lipid:organic normalization of BSAFs to be helpful in describing the observed order of magnitude variation in the non-normalized BSAFs. This finding was confirmed by comparing probability distributions for non-normalized BSAFs to the $BSAF_{lipid,oc}$ distributions (Figure 3, plus additional plots for all the PCB homologs and PCDD/F congeners in Tables A-1 through A-3 of the appendix). As shown, lipid:organic carbon normalization of BSAFs did not explain the order of magnitude variations that were previously shown in Figure 2. However, lipid:organic carbon normalization did remove deviations from log normal trendlines that were previously noted for the highest 4 or 5 BSAFs on the non-normalized BSAF plots.

The potential effects of chemical properties on BSAF were evaluated graphically by plotting the geometric mean $\pm$ one log standard deviation for the PCB homolog and the PCDD/F congener BSAFs versus log K_{ow}. As shown by the blue circles in Figure 4, BSAFs for the PCB homologs increased with increasing log K_{ow} for the less chlorinated homologs and then levelled off at a value of approximately 0.15 kg dry wt / kg wet wt for the more chlorinated homologs. Similar behavior is shown for PCB congeners by the smaller gray circles. However, computed BSAFs for the PCB congeners show more variability. This was particularly apparent for the lower K_{ow} congeners where BSAF variations appeared to be related to the number of ortho-substituted chlorines on the biphenyl structure.

For comparison, BSAFs for PCDDs (red diamonds) and PCDFs (green triangles) appeared to be much lower than BSAFs for PCBs with equivalent log K_{ow} values. For example, BSAF values for the tetra- and penta-CDD/F congeners (with log K_{ow}'s of 6-7) were approximately 0.05 kg dry wt / kg wet wt, which is approximately 3 times lower than BSAFs for PCBs with comparable log K_{ow}'s. For the higher chlorinated PCDDs and PCDFs, BSAFs did not show a leveling-off but rather exhibited a significant decline with increasing log K_{ow}.

More detailed evaluations of bioaccumulation behavior: More detailed evaluations of bioaccumulation were performed by separately considering sediment-water partitioning (K_p's) and organism-water

partitioning (BAFs). Calculations of log K_p and log BAF were performed using the 20 sediment samples with measured porewater concentrations and are presented graphically in Figure 5.

As shown in Figure 5a, log K_p values for the less chlorinated PCBs are relatively constant with log K_p equal to approximately 5. Log K_p values for the more chlorinated PCBs are shown to increase proportionally with increasing log K_{ow} values. Log K_p values for the PCDD congeners appear to be similar or be slightly below the log K_p values for the more chlorinated PCBs. However, log K_p values for the PCDF congeners are higher than the log K_p values for PCBs. Similar behavior was previously observed by Barring et al. (2002) where they reported greater sorption of PCDFs (and PAHs) to NIST diesel soot particles compared to sorption of PCBs and PCDDs with similar log K_{ow} values.

In contrast to the log K_p results, log BAFs for PCBs were found to increase with increasing log K_{ow} over the full range of log K_{ow} values (Figure 5b). Log BAFs for PCDFs were closely aligned to the PCB results. However, the log BAFs for PCDD congeners showed only a slight increase with increasing log K_{ow}. This result suggests that: (i) the more chlorinated PCDD congeners may be metabolized by the bioaccumulation test organism*, N. virens,* or (ii) the bulkier PCDD congeners (with two oxygen bridges connecting the benzene rings) may be less effectively transferred through biological membranes. The latter explanation is more likely since invertebrates like *N. virens* are believed to lack the p450 enzyme pathway which has been identified in metabolizing chlorinated dioxins and dioxin-like PCB congeners.

Development of K_p, BAF and BSAF relationships: A final step in this task was to develop relationships for K_p, BAF and BSAF as a function of sediment, organism and chemical properties. The initial focus of these evaluations was on PCB congeners because: (i) PCBs cover a wide range of log K_{ow} values, and (ii) more reliable estimates are available for PCB chemical parameters (e.g., log K_{ow}, ΔH_{ow}, K^{salt}, dihedral angle).

Various relationships have been proposed to describe sediment-water partitioning of hydrophobic organic contaminants in terms of the sediment amorphous organic carbon content ($f_{oc} = f_{TOC} - f_{BC}$), the sediment black carbon content (f_{BC}), chemical hydrophobicity (as represented by log K_{ow}) and the chemical porewater concentrations (Gustafsson et al. 1997; Accadi-Dey and Gschwend 2002, 2003). This approach was subsequently extended by Greene et al. (2013) by including the dihedral angle to account for observed differences in binding that were attributed to the number of ortho chlorines on the biphenyl structure.

After testing various relationships based on f_{aoc}, f_{BC}, K_{ow}, C_{pw} and the dihedral angle, a best fit to the observed K_p values for PCB congeners was obtained using the following two coefficient relationship:

$$K_p = \beta_1 f_{aoc} K_{ow} + a_1 f_{BC}(90° - dihedral\ angle) \quad \text{(Eq. 11)}$$

As noted previously, values for the two model coefficients (β_1, a_1) were obtained by minimizing the sum of the squares of the 'log K_p (model) – log K_p (observed)' residuals using SOLVER in Microsoft EXCEL. In these evaluations, one PCB congener—PCB #89 (2,2',3,4,6' pent-CB), appeared as an outlier and was not included in the K_p model fitting evaluations. Inclusion of other parameters; e.g., the porewater

concentration in the black carbon portion of the K_p relationship which has been considered by other investigators, did not provide a noticeable improvement in the K_p model fit.

An example for the K_p model fit is shown in Figure 6a for a sediment sample from Elizabeth Channel (EC-IC-2-L). Model coefficients for sample EC-IC-2-L are given as $\beta_1 = 1.04$ and $a_1 = 1.57 \times 10^6$. The five model lines (and corresponding datapoints) on Figure 6a are related to the number of ortho-substituted chlorines on the PCB congeners. Results for congeners with '0' ortho-substituted chlorines, which are most able to distort into a planar configuration, exhibited the strongest binding to black carbon and hence have the highest log K_p values. As the number of ortho-substituted chlorines increase, log K_p values are shown to decrease accordingly. Finally, the five model lines merge at higher log K_{ow} values indicating binding of PCBs to sediments is expected to become more dependent on partitioning to amorphous organic matter (f_{aoc}) as log K_{ow} increases.

A global fit of the K_p model was obtained using PCB congener data for the 20 sediment samples with PCB porewater measurements. The two model coefficients for the global fit to the 20 sediment samples are given as: $\beta_1 = 1.2$ and $a_1 = 8.76 \times 10^5$. Based on these values, the standard deviation of the 'log K_p (model) – log K_p (observed)' residuals is given as 0.286, which indicates the 71% of the calculated K_p values were within a factor of 2 of the observed K_p values. These results are presented graphically in Figure 6b as a log K_p calculated versus log K_p observed cross-plot.

Similar calculations were performed in developing a BAF relationship for the PCB congeners. A best fit to the observed BAFs for PCBs was obtained using the simple one coefficient relationship below:

$$BAF = \beta_2 f_{lipid} K_{ow} \qquad \text{(Eq. 12)}$$

where the value for β_2 was obtained by minimizing the sum of the squares of the 'log BAF (model) – log BAF (observed)' residuals using SOLVER in Microsoft EXCEL. In addition to PCB #89 (cited above), three lower chlorinated congeners—PCB #5 (2,3 di-CB), PCB #6 (2,3'-di-CB) and PCB #16 (2,2',3 tri-CB), also appeared as outliers and were excluded from BAF model evaluations.

An example for the BAF model fit is shown in Figure 7a for a sediment sample from Elizabeth Channel (EC-IC-2-L). As shown, a close correspondence of observed and calculated BAFs was obtained using a β_2 value of 0.284 for the EC-IC-2-L sediment sample. A global fit of the BAF model was obtained for the 20 sediment samples with PCB porewater measurements using a β_2 value of 0.253. The standard deviation of the 'log BAF (model) – log BAF (observed)' residuals is given as 0.318, which indicates the 66% of the calculated BAF values were within a factor of 2 of the observed BAF values. These results are presented graphically in Figure 7b as a log BAF calculated versus log BAF observed cross-plot.

The K_p and BAF relationships given above were combined into an equation for BSAF as:

$$BSAF = \frac{BAF}{K_p} = \frac{\beta_2 f_{lipid} K_{ow}}{\beta_1 f_{aoc} K_{ow} + a_1 f_{BC}(90° - dihedral\ angle)} \qquad \text{(Eq. 13)}$$

An example for the BSAF model fit is shown in Figure 8a for a sediment sample from Elizabeth Channel (EC-IC-2-L) using the EC-IC-2-L fitting coefficients: β_2=0.284, β_1 = 1.04 and $a_1 = 1.57 \times 10^6$. The five model lines (and corresponding datapoints) on Figure 8a are related to the number of ortho-substituted chlorines on the biphenyl structure. For log K_{ow} < 7, the lower BSAFs for PCBs with '0' ortho-substituted chlorines are attributed to the strong binding of the '0' ortho-substituted PCBs to black carbon. As the number of ortho-substituted chlorines increase, the BSAF values are shown to decrease accordingly. For log K_{ow} > 7, the five model lines merge indicating binding of PCBs to sediments is expected to become more dependent on partitioning to amorphous organic matter (f_{aoc}) as log K_{ow} increases.

The BSAF results for the 20 sediment samples with PCB porewater measurements are shown in Figure 8b as a BSAF (calculated) versus BSAF (observed) cross-plot. Coefficients used in these calculations are based on global model fits: β_2 = 0.253, β_1 = 1.2 and $a_1 = 8.76 \times 10^5$. The standard deviation of the 'log BSAF (calculated) – log K_p (observed)' residuals is given as 0.349, which indicates the 61% of the calculated K_p values were within a factor of 2 of the observed K_p values. A closer look at the results revealed that the largest differences in BSAF (calculated) and BSAF (observed) results were associated with four of the off-channel sediment samples. These included two samples from Port Jersey (PJ-OC-2-S, PJ-OC-2-L) where model calculations underpredicted observed BSAFs, and one sample from Elizabeth Channel (EC-OC-2-S) and one sample from Port Newark Channel (PNC-OC-1-L) where model calculations overpredicted observed BSAFs. The BSAF (calculated) versus BSAF (observed) cross-plot for the four off-channel sediment samples is shown in Figure 8c, and the cross-plot for the remaining sediments (which included six off-channel and ten in-channel samples) is presented in Figure 8d.

BSAF plots for PCB homologs as a function of log K_{ow} are presented in Figure 9 for the Port Jersey, Elizabeth Channel and Port Newark Channel off-channel samples, along with BSAFs for Buttermilk Channel in-channel samples. The two Port Jersey samples cited above (PJ-OC-2-S, PJ-OC-2-L) showed very high BSAFs for PCB homologs with log K_{ow}'s > 6.5 (Figure 9a). As shown in Figure 9b, similar behavior was also observed in two sediment samples from Buttermilk Channel (BMC-IC-2-S, BMC-IC-2-L), indicating that enhanced PCB bioaccumulation was not limited to off-channel sediments. Enhanced PCB bioaccumulation of the higher K_{ow} PCB homologs was also noted in several of the CARP 1 field-collected samples from the outer harbor sites (HydroQual 2007; Landeck Miller et al. 2011).

A detailed two-box bioaccumulation model was developed to examine enhanced PCB bioaccumulation that has been observed in the four CARP II laboratory bioaccumulation tests and in several of the CARP 1 field-collected worms (see Appendix C). Model results show that enhanced bioaccumulation of the higher chlorinated PCBs is likely attributed to dietary uptake which has been shown to depend on organism growth rates. However, organism growth rates for individual CARP II bioaccumulation tests were not available to apply the detailed two-box bioaccumulation model.

In contrast to the BSAF results cited above for Port Jersey and Buttermilk Channel, very low BSAFs were observed for the Elizabeth Channel (EC-OC-2-S) and Port Newark Channel (PNC-OC-1-L) samples (Figure 9c,d). BSAF model calculations with the global fitting parameters consistently overpredicted the observed

BSAFs for these two sediment samples. Chronic toxicity may be a plausible explanation, particularly for the PNC-OC-1-L sample which had the highest concentrations of PCBs and PCDD/Fs.

Finally, the PCB model equations for K_p, BAF and BSAF were applied to PCDD/Fs by considering PCDD/F congeners to be co-planar (i.e., with the dihedral angel set equal to '0'). The model coefficients for these evaluations were based on global PCB model fits for the 20 stations with porewater measurements: β_2 = 0.253, β_1 = 1.2 and $a_1 = 8.76 \times 10^5$. Comparison of the K_p model calculations to observed geometric means ($\pm$ one log standard deviation) are presented in Figure 10a. As shown, observed K_p values for PCDDs are slightly below but within a factor of two of the model calculations. The observed K_p values for the tetra- and penta-CDFs are also in line with model calculations. However, observed K_p's for the more chlorinated PCDF congeners are well above the model calculations.

A similar comparison of BAF model calculations to observed geometric means ($\pm$ one log standard deviation) are presented in Figure 10b. As shown, the observed BAFs for PCDD are relatively flat compared to model calculations that show a proportional increase in BAFs with increasing K_{ow} values. This is in contrast to the observed BAFs for PCDFs, which are closely aligned to model calculations over the full range of log K_{ow} values.

Final comparisons for BSAFs (Figure 10c) show that the observed BSAFs for tetra- and penta-CDD/Fs are within a factor of two (or slightly below a factor of two) of the model calculations. Observed BSAFs for both the more chlorinated PCDDs and PCDFs show a steady decrease with increasing log K_{ow} and fall well below the model calculations. However, the underlying causes for the observed decreases in BSAFs are quite different for PCDDs and PCDFs. For PCDD, the decrease in BSAFs with increasing log K_{ow} is likely associated with limited uptake of the bulkier PCDD congeners through biological membranes. For PCDF, the decrease in BSAFs with increasing log K_{ow} is more likely attributed to stronger binding (or possibly encapsulation) of the more chlorinated PCDFs in black carbon.

Conclusions

As part of the CARP II investigations, 68 sediment samples that were collected from various locations in NY-NJ Harbor. For total PCB evaluations, 28-day bioaccumulation tests were used along with EPA Region 2 protocols of multiplying 28-day results by a factor of two to estimate steady-state concentrations. Based on the steady-state results, four of the CARP II sediment samples exceeded the Total PCB dredged material management guidelines for HARS disposal (113 ppb). For 2,3,7,8-TCDD evaluations (based directly on 28-day bioaccumulation test results), the HARS disposal guideline of 1 ppt was exceeded for all sediment samples from Port Newark Channel and for several sediment samples from Elizabeth Channel. Finally, the HARS disposal guideline for Total TEQs (4.5 ppt) was exceeded in one off-channel sediment sample from Port Newark Channel.

CARP II bioaccumulation test results were used in calculating median and 90th percentile BSAFs for PCB homologs and PCDD/F congeners. Results are presented in Table 1 in terms of 28-day BSAFs. The 90th percentile values from the CARP II bioaccumulation tests were found to be roughly within a factor of two of the EPA Region 2 recommended values for tetra-, hexa- and octa-CBs and of 2,3,7,8-TCDD. The 90th

percentile value for di-CB however were found to be 13 times lower than the EPA Region 2 recommended value. Although this difference in the di-CB BSAF values is large, it is not considered a major concern because di-CB accounts for a relatively small portion of total PCBs that accumulate in the organism.

Sediment-water partitioning (K_p), organism-water partition (BAF) and biota-sediment accumulation (BSAF) for PCBs were related to sediment, organism and chemical properties. Final relationships are given in Eq. 11-13. The three model coefficients were determined using PCB congener data from the 20 sediment samples with porewater measurements and are given as: $\beta_2 = 0.253$, $\beta_1 = 1.2$ and $a_1 = 8.76 \times 10^5$.

K_p model results show that PCBs with 0 or 1 chlorine in the ortho position bind more strongly to black carbon. These congeners (which are more likely to be present in the less chlorinated homolog groups) have a stronger affinity to partition to sediments. This effect largely explains the higher K_p, and concomitantly, the lower BSAF values that are observed for the lower chlorinated homolog groups.

Application of the PCB model equations for K_p, BAF and BSAF to PCDD/Fs showed mixed results. The PCB model provided reasonable estimates (to within roughly a factor of two) for tetra- and penta-CDD/Fs. However, the PCB model equations did not provide an adequate description of BSAFs for the more chlorinated PCDD/F congeners, which showed a continuous decrease in BSAFs with increasing K_{ow}. Reasons for the decreasing BSAFs are likely attributed to: (i) lower BAFs for PCDDs due to limited uptake of the bulkier PCDD congeners through biological membranes, and (ii) higher K_p's for PCDFs due to stronger binding (or possibly encapsulation) of the more chlorinated PCDFs in black carbon.

Further studies should be considered to: (i) confirm the underlying causes for the very high BSAFs and the very low BSAFs that were observed for PCBs in a few of the sediment samples, (ii) examine how differences in chemical structure (particularly planarity and molecular size) affect K_p and BAF behavior of PCDDs and PCDFs, and (iii) evaluate how BSAFs for CARP II harbor sediment samples relate to bioaccumulation at the HARS.

References

Accardi-Dey AM, Gschwend PM. 2003. Reinterpreting literature sorption data considering both absorption into organic carbon and adsorption onto black carbon. T2 - Environmental Science and Technology. 37(1):99-106. doi:10.1021/es020569v.

Accardi-Dey AM, Gschwend PM. 2002. Assessing the combined roles of natural organic matter and black carbon as sorbents in sediments. Environmental Science and Technology. 36(1):21-29. doi:10.1021/es010953c.

Bucheli TD, Broman D, Orjan Gustafsson O. Soot-water distribution coefficients for polychlorinated dibenzo-p-dioxins, polychlorinated dibenzofurans and polybrominated diphenylethers determined with the soot cosolvency-column method

Burkhard LP, Mount DR, Highland TL, Hockett JR, Norberg-King Billa N, Hawthorne SB, Miller DJ, Grabanski CB. 2013. Evaluation of PCB bioaccumulation by Lumbriculus variegatus in field-collected sediments. Environmental Toxicology and Chemistry. 32(7)1495-1503. doi:10.1002/etc.2207.

Cornelissen G, Wiberg K, Broman DAG, Arp, HPH, Persson Y, Sundqvist K, Jonsson P. 2008. Freely dissolved concentrations and sediment-water activity ratios of PCDD/Fs and PCBs in the open Baltic sea. Environmental Science and Technology. 42(23):8733-8739. doi:10.1021/es8018379.

Dunn WJ, Koehler M, Stalling DL, Schwartz TR. 1986. Relationship between gas chromatographic retention of polychlorinated dibenzofurans and calculated molecular surface area. Analytical Chemistry. 58(8):1835-1838.

Farley KJ, Thomann RV, Cooney III TF, Damiani DR, Wands JR. 1999. Fate and Bioaccumulation of Toxic Contaminants in New York-New Jersey Harbor. Final Report to the Hudson River Foundation, New York, NY.

Friedman CL, Burgess RM, Perron MM, Cantwell MG, Ho KT, Lohmann R. 2009. Comparing polychaete and polyethylene uptake to assess sediment resuspension effects on PCB bioavailability. Environmental Science and Technology. 43(8)2865-2870. doi:10.1021/es803695n

Friesen KJ, Webster GRB. 1990. Temperature dependence of the aqueous solubilities of highly chlorinated dibenzo-p-dioxins. Environmental science & technology. 24:97-101

Greene RW, Di Toro DM, Farley KJ, Phillips KL, Tomey C. 2013. Modeling water column partitioning of polychlorinated biphenyls to natural organic matter and black carbon. Environmental Science and Technology. 47(12)6408-6414. doi:10.1021/es400817c.

Gustafsson Ö, Haghseta F, Chan C, MacFarlane J, Gschwend PM. 1997. Quantification of the Dilute Sedimentary Soot Phase: Implications for PAH Speciation and Bioavailability. Environmental Science and Technology. 31(1)203-209.

Hawker DW, Connell DW. 1988. Octanol-water partition coefficients of polychlorinated biphenyl congeners. Environmental science and technology. 22(4):382-387.

HydroQual, Inc. 2007. A Model for the Evaluation and Management of Contaminants of Concern in Water, Sediment, and Biota in the NY/NJ Harbor Estuary: Contaminant Fate and Transport and Bioaccumulation Sub-models. Final Report to the Hudson River Foundation, New York, NY.

Lambert MK, Friedman C, Luey P, Lohmann R. 2011. Role of black carbon in the sorption of polychlorinated dibenzo-p-dioxins and dibenzofurans at the diamond alkali superfund site, Newark Bay, New Jersey. Environmental Science and Technology. 45(10)4331-4338. doi:10.1021/es103953t.

Landeck Miller RE, Farley KJ, Wands JR, Santore R, Redman AD, Kim NB. 2011. Fate and transport modeling of sediment contaminants in the New York/New Jersey Harbor Estuary." *Urban Habitats* 6.http://www.urbanhabitats.org/v06n01/fateandtransport_full.html.

Landeck Miller, RE, Farley KJ, De Rosa L, Kogan N, Rugabandana R, Wands JR. 2023. CARP Models Future Projection Scenarios. HDR report for NY/NJ Harbor Contamination Assessment and Reduction Project, CARP II, New Jersey Department of Transportation, Under Agreement with Monmouth University and the Hudson River Foundation.

Lohmann R, MacFarlane JK, Gschwend PM. Importance of Black Carbon to Sorption of Native PAHs, PCBs, and PCDDs in Boston and New York Harbor Sediments. Environmental Science and Technology. 39(1):141-148. doi:10.1021/es049424

McLeod PB, Van Den Heuvel-Greve MJ, Luoma SN, Luthy RG. 2007. Biological uptake of polychlorinated biphenyls by Macoma balthica from sediment amended with activated carbon. Environmental Toxicology and Chemistry. 26(5):980-987. doi:10.1897/06-278R1.1

Mackay D, Shiu WY, Ma KC. 1992. Illustrated Handbook of Physical and Environmental Fate for Organic Chemicals. Volume II: Polynuclear Aromatic Hydrocarbons, Polychlorinated Dioxins and Dibenzofurans. Lewis Publishers, Chelsea, MI.

Sacan MT, Özkul M. Erdem, SS. 2005. Physico-chemical properties of PCDD/PCDFs and phthalate esters. SAR and QSAR in Environmental Research. 16(5)443-459.

Ulrich N, Endo S, Brown TN, Watanabe N, Bronner G, Abraham MH, Goss K-U. 2017. UFZ-LSER database v 3.2 [Internet]. http://www.ufz.de/lserd

USACE New York District / USEPA Region 2. 2016. Guidance for Performing Tests on Dredged Material Proposed for Ocean Disposal. New York, NY.

Table 1. Summary of PCB homolog probability distributions. Median and 90th percentile for 28-day BSAF values were calculated using the following regression equation: log BSAF = slope × Z-score + intercept (where the 90th percentile corresponds to a Z-score of 1.28). BSAF values are reported in terms of kg sediment dry weight per kg organism wet weight. The current EPA Region 2 dredged material guidance values are presented for comparison. Median, 90th percentile and guideline BSAF values are reported in terms of kg sediment dry weight per kg organism wet weight.

	Slope	Intercept	Median[(a)]	90th percentile[(a)]	Current Dredged Material Guidance
mono-CB	0.323	-2.776	0.0017	0.0043	
di-CB	0.236	-2.042	0.0091	0.0182	0.243
tri-CB	0.285	-1.667	0.0215	0.0499	
tetra-CB	0.232	-1.196	0.0637	0.1261	0.300
penta-CB	0.223	-0.934	0.1164	0.2248	
hexa-CB	0.252	-0.724	0.1888	0.3968	0.496
hepta-CB	0.266	-0.729	0.1868	0.4091	
octa-CB	0.283	-0.842	0.1440	0.3315	0.216
nona-CB	0.273	-0.859	0.1382	0.3093	
deca-CB	0.258	-0.936	0.1159	0.2480	
total PCBs	0.219	-1.093	0.0807	0.1540	

[(a)] Median and 90th percentile BSAF values were calculated using the following regression equation: log BSAF = slope × Z-score + intercept (where the 90th percentile corresponds to a Z-score of 1.28).

Table 2. Summary of polychlorinated dibenzodioxin and ploy-chlorinated dibenzofuran probability distributions. Median and 90th percentile for 28-day BSAF values were calculated using the following regression equation: log BSAF = slope × Z-score + intercept (where the 90th percentile corresponds to a Z-score of 1.28). The current EPA Region 2 dredged material guidance value for 2,3,7,8-TCDD is presented for comparison. Median, 90th percentile and guideline BSAF values are reported in terms of kg sediment dry weight per kg organism wet weight.

	Slope	Intercept	Median[(a)]	90th percentile[(a)]	Current Dredged Material Guidance
2,3,7,8-TCDD	0.217	-1.450	0.0355	0.0674	0.052
1,2,3,7,8-PECDD	0.295	-1.279	0.0526	0.1255	
1,2,3,4,7,8-HXCDD					
1,2,3,6,7,8-HXCDD	0.270	-1.780	0.0166	0.0368	
1,2,3,7,8,9-HXCDD	0.299	-1.942	0.0114	0.0276	
1,2,3,4,6,7,8-HPCDD	0.258	-2.300	0.0050	0.0107	
OCDD	0.259	-2.650	0.0022	0.0048	
2,3,7,8-TCDF	0.203	-1.350	0.0446	0.0812	
1,2,3,7,8-PECDF	0.253	-1.376	0.0421	0.0888	
2,3,4,7,8-PECDF	0.237	-1.406	0.0392	0.0789	
1,2,3,4,7,8-HXCDF	0.310	-1.808	0.0156	0.0388	
1,2,3,6,7,8-HXCDF	0.306	-1.893	0.0128	0.0316	
1,2,3,7,8,9-HXCDF					
2,3,4,6,7,8-HXCDF	0.388	-1.824	0.0150	0.0471	
1,2,3,4,6,7,8-HPCDF	0.310	-2.266	0.0054	0.0135	
1,2,3,4,7,8,9-HPCDF					
OCDF	0.340	-2.506	0.0031	0.0085	

[(a)] Median and 90th percentile BSAF values were calculated using the following regression equation: log BSAF = slope × Z-score + intercept (where the 90th percentile corresponds to a Z-score of 1.28).

Table 3. Correlation coefficients relating 28-day BSAFs for PCB homologs to total organic carbon (f_{TOC}), lipid content (f_{Lipid}) and soot content (f_{Soot}),and the lipid:TOC ratio (f_{Lipid}/f_{TOC}).

Homolog	Name	f_{TOC}	f_{Lipid}	f_{Soot}	f_{Lipid} / f_{TOC}
1	mono-CB	-0.53	0.15	0.32	0.48
2	di-CB	-0.49	0.12	0.25	0.45
3	tri-CB	-0.62	0.03	0.18	0.46
4	tetra-CB	-0.67	0.07	0.18	0.54
5	penta-CB	-0.56	0.02	0.15	0.46
6	hexa-CB	-0.50	-0.03	0.19	0.38
7	hepta-CB	-0.47	-0.02	0.25	0.35
8	octa-CB	-0.48	-0.01	0.30	0.36
9	nona-CB	-0.48	-0.06	0.28	0.34
10	deca-CB	-0.48	-0.06	0.28	0.35
	Total PCBs	-0.62	0.02	0.31	0.49

Note: correlation coefficients of 0 – 0.3 represent a weak correlation, 0.3 – 0.7 represent a moderate correlation, 0.7 – 1.0 represents a strong correlation of BSAF values to the various measures.

Table 4. Correlation coefficients relating 28-day BSAFs for 2,3,7,8-chlorine substituted PCDD/F to total organic carbon (f_{TOC}), lipid content (f_{Lipid}) and soot content (f_{Soot}),and the lipid:TOC ratio (f_{Lipid}/f_{TOC}).

Congener	Name	f_{TOC}	f_{Lipid}	f_{Soot}	f_{Lipid} / f_{TOC}
1	2,3,7,8-TCDD	-0.28	0.14	0.30	0.30
2	1,2,3,7,8-PECDD	-0.38	0.09	0.27	0.27
3	1,2,3,4,7,8-HXCDD	-0.26	-0.04	0.18	0.18
4	1,2,3,6,7,8-HXCDD	-0.29	0.11	0.38	0.38
5	1,2,3,7,8,9-HXCDD	-0.32	0.10	0.33	0.33
6	1,2,3,4,6,7,8-HPCDD	-0.16	0.09	0.41	0.41
7	OCDD	-0.22	0.06	0.42	0.42
8	2,3,7,8-TCDF	-0.33	0.06	0.26	0.26
9	1,2,3,7,8-PECDF	-0.50	0.01	0.19	0.19
10	2,3,4,7,8-PECDF	-0.42	0.06	0.22	0.22
11	1,2,3,6,7,8-HXCDF	-0.33	0.04	0.26	0.26
12	1,2,3,4,7,8-HXCDF	-0.33	0.05	0.29	0.29
13	1,2,3,7,8,9-HXCDF	-0.56	-0.01	-0.26	-0.26
14	2,3,4,6,7,8-HXCDF	-0.30	-0.04	0.22	0.22
15	1,2,3,4,6,7,8-HPCDF	-0.19	0.04	0.35	0.35
16	1,2,3,4,7,8,9-HPCDF	-0.34	-0.14	0.18	0.18
17	OCDF	-0.12	0.00	0.30	0.30

Note: correlation coefficients of 0 – 0.3 represent a weak correlation, 0.3 – 0.7 represent a moderate correlation, 0.7 – 1.0 represents a strong correlation of BSAF values to the various measures.

(a)

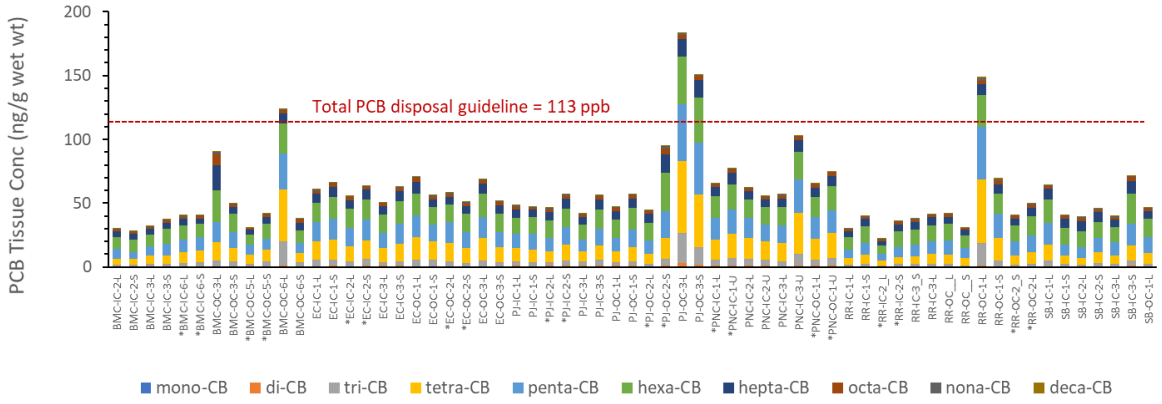

(b)

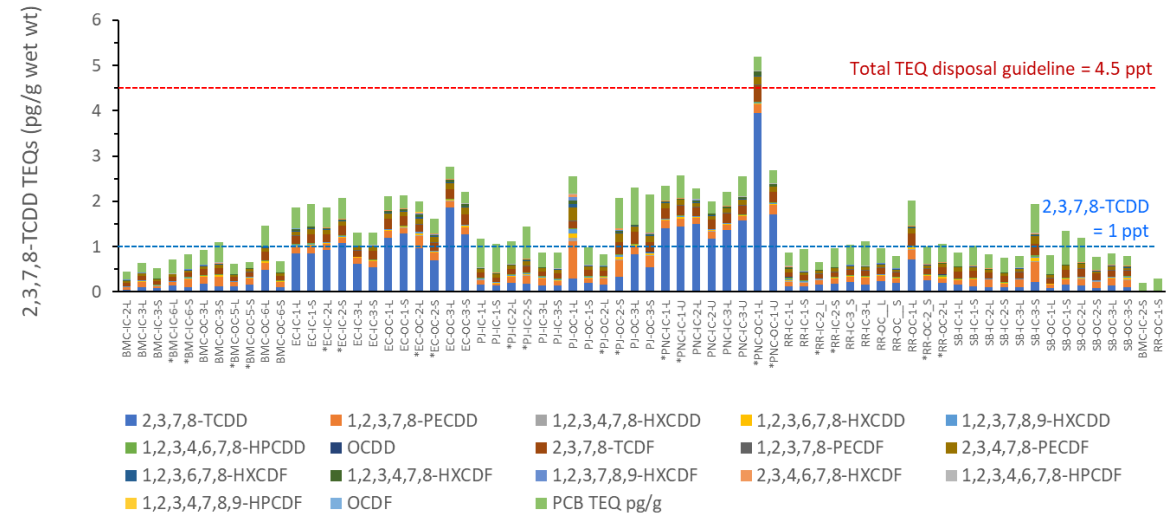

Figure 1. CARP II estimates of tissue concentrations in *N. virens* for (a) PCB homologs and (b) 2,3,7,8-TCDD Toxic Equivalents (TEQs). Results are presented for 68 sediment samples that were collected throughout NY-NJ Harbor. PCB results were obtained by multiplying 28-day bioaccumulation test results by a factor of 2 (Figure 1a). TEQ results were determined directly from the 28-day bioaccumulation results without adjustment to steady state (Figure 1b). Current dredged material management guidelines for HARS disposal are also presented on the figure for comparison to the bioaccumulation results. (Note: PCDD/F measurements were not given for two of the 68 samples: BMC-IC-2-S and RR-OC-1-S.)

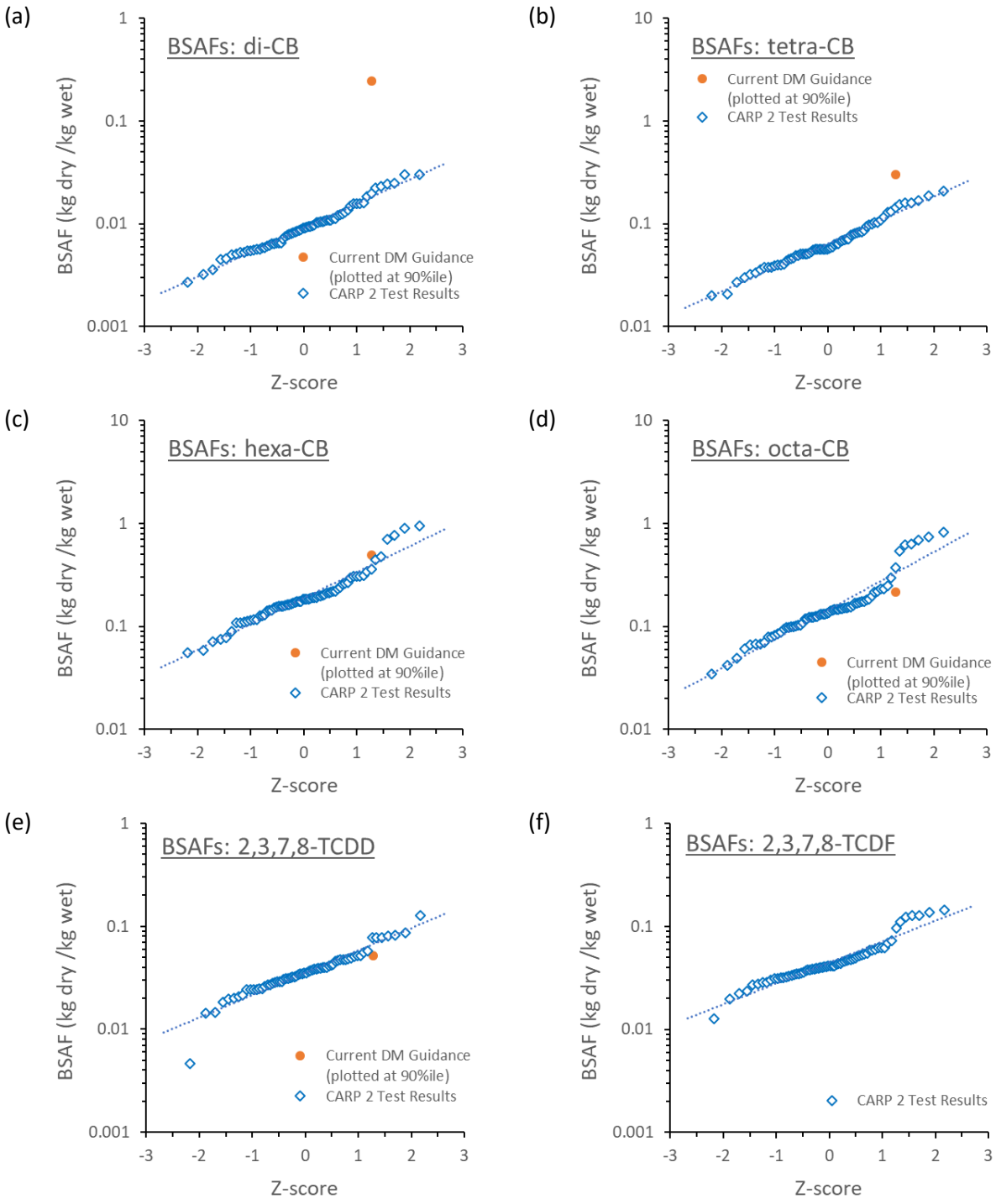

Figure 2. 28-day BSAF results for 68 sediment samples are presented as probability distributions for several PCB homologs and PCDD/F congeners. EPA Region 2 recommended BSAF values that are currently used in dredged material evaluations are also included for the PCB homologs and for 2,3,7,8-TCDD. The EPA BSAF estimates were purposely plotted with a Z-score corresponding to the 90th percentile.

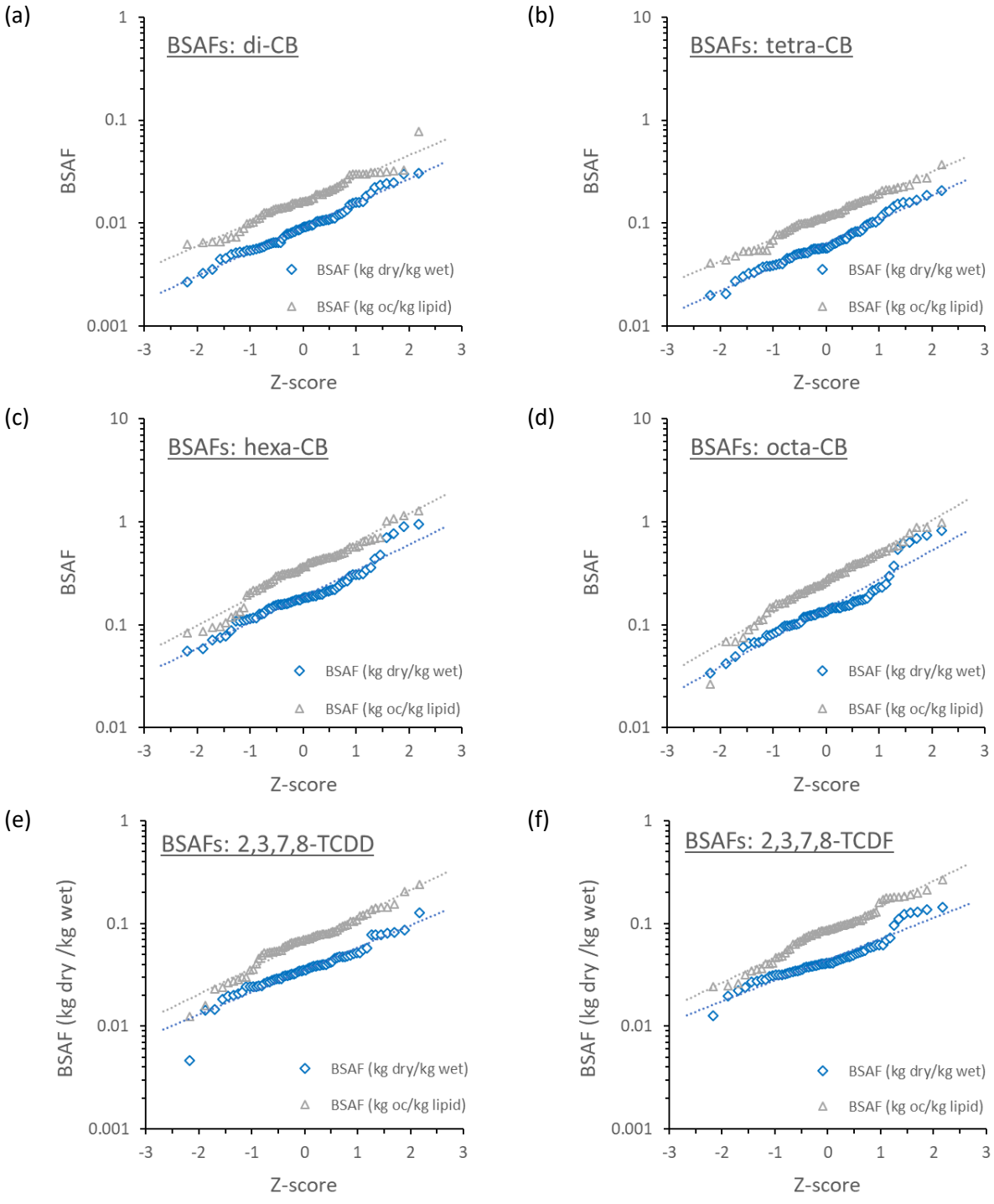

Figure 3. Comparison of lipid:organic normalization of 28-day BSAF and non-normalized 28-day BSAF probability distributions for several PCB homologs and PCDD/F congeners. Plots for additional PCB homologs and PCDD/F congeners is given in the appendix.

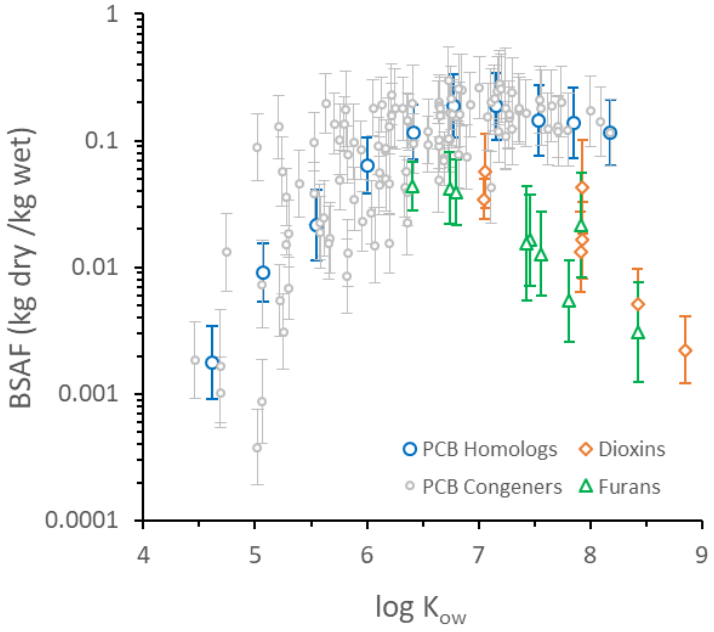

Figure 4. 28-day BSAFs (plotted as geometric means ± one log standard deviation) for PCB homologs, PCB congeners, PCDD congeners and PCDF congeners versus log K_{ow} for the 68 CARP II sediment samples that were collected from various locations throughout NY-NJ Harbor. (Note: PCDD/F measurements were not given for two of the 68 samples: BMC-IC-2-S and RR-OC-1-S.)

(a)

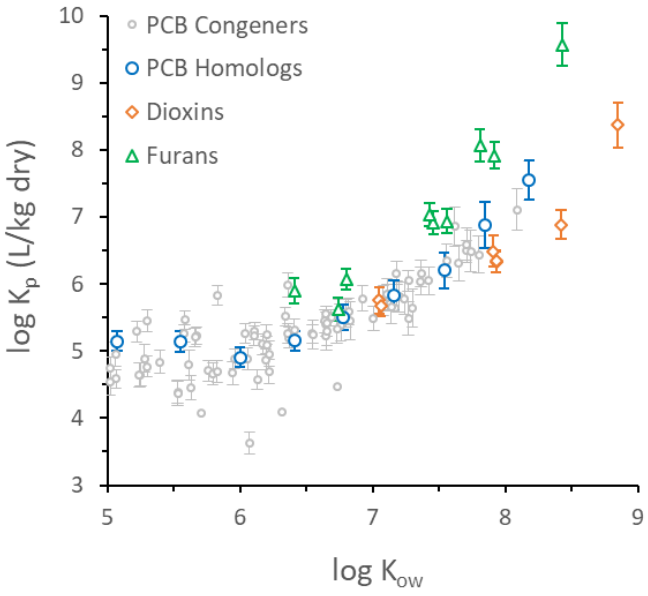

(b)

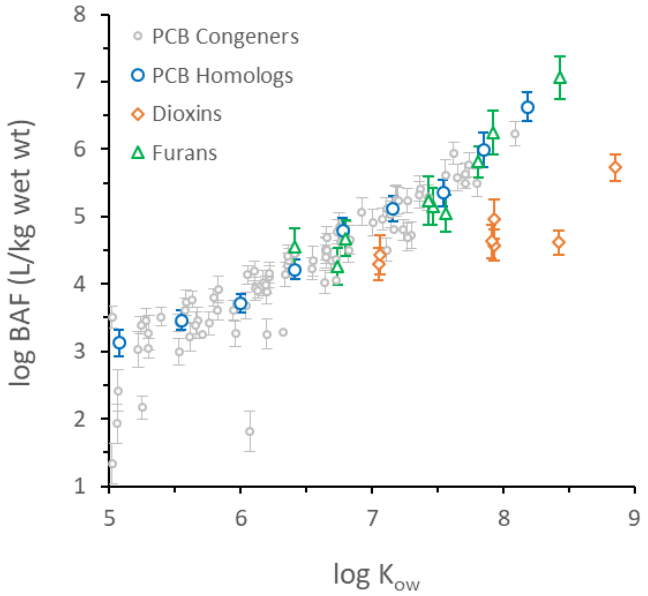

Figure 5. log K_p's and log BAFs (plotted as geometric means ± one log standard deviation) for PCB homologs, PCB congeners, PCDD congeners and PCDF congeners versus log K_{ow} for the 20 sediment samples with measured porewater concentrations.

(a)

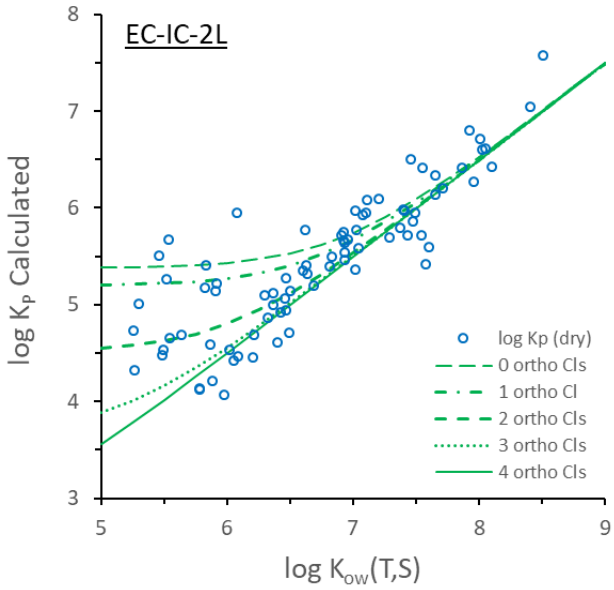

(b)

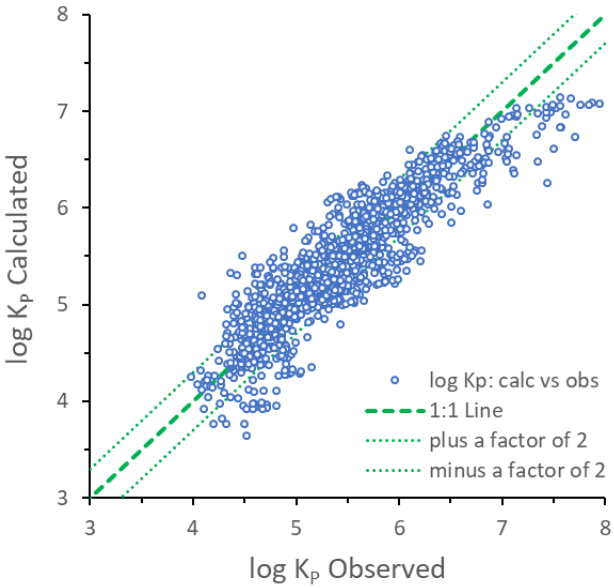

Figure 6. (a) K_p model fit for sediment sample EC-IC-2-L from Elizabeth Channel based on Equation 11 and the following model coefficients: $\beta_1 = 1.04$ and $a_1 = 1.57 \times 10^6$. (b) log K_p calculated versus log K_p observed cross-plot based Equation 11 and the following model coefficients that were obtained from the global fit of the K_p model for the 20 sediment samples with PCB porewater measurements: $\beta_1 = 1.2$ and $a_1 = 8.76 \times 10^5$.

(a)

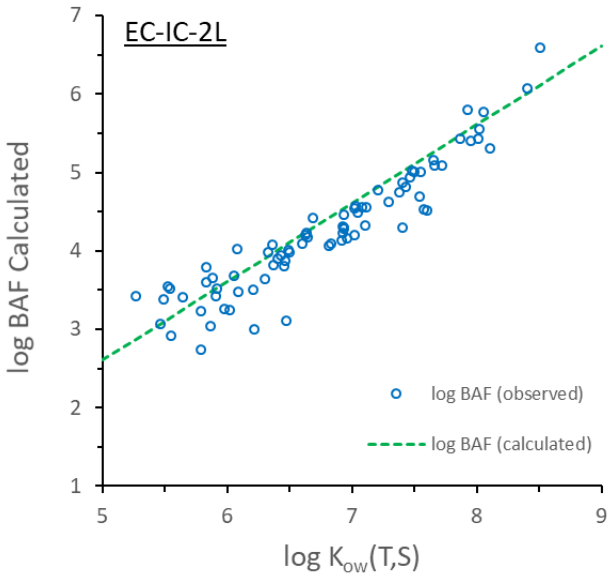

(b)

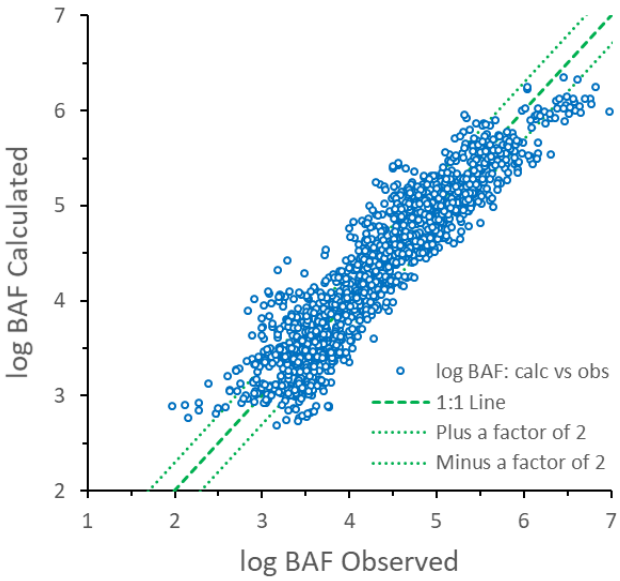

Figure 7. (a) BAF model fit for sediment sample EC-IC-2-L from Elizabeth Channel based on Equation 12 and the following model coefficient: $\beta_2 = 0.284$. (b) log BAF calculated versus log BAF observed cross-plot based Equation 12 and the following model coefficients that were obtained from the global fit of the BAF model for the 20 sediment samples with PCB porewater measurements: $\beta_2 = 0.253$.

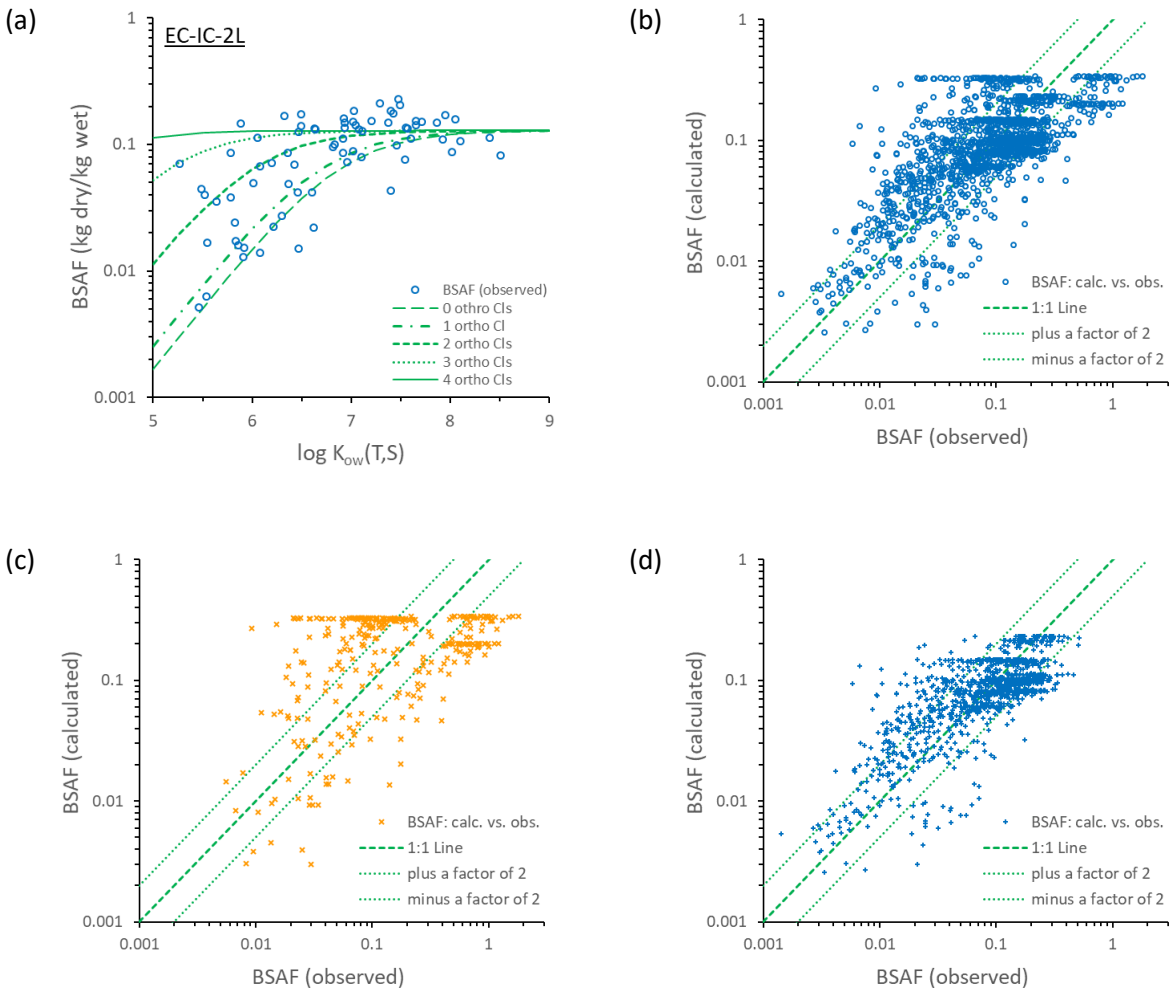

Figure 8. (a) BSAF model fit for sediment sample EC-IC-2-L from Elizabeth Channel based on Equation 12 and the following model coefficient: β_2=0.284, β_1 = 1.04 and a_1 = 1.57 $\times$ 10^6. (b) Calculated versus observed BSAF cross-plot based Equation 13 and the following model coefficients that were obtained from the global fit of the K_p and BAF model for the 20 sediment samples with PCB porewater measurements: β_2 = 0.253, β_1 = 1.2 and a_1 = 8.76 $\times$ 10^5. (c) Calculated versus observed BSAF cross-plot for the four off-channel sediment samples (PJ-OC-2-S, PJ-OC-2-L, EC-OC-2-S, PNC-OC-1-L) that had the largest differences in BSAF (calculated) and BSAF (observed) results. (d) Calculated versus observed BSAF cross-plot for the other 16 sediment samples.

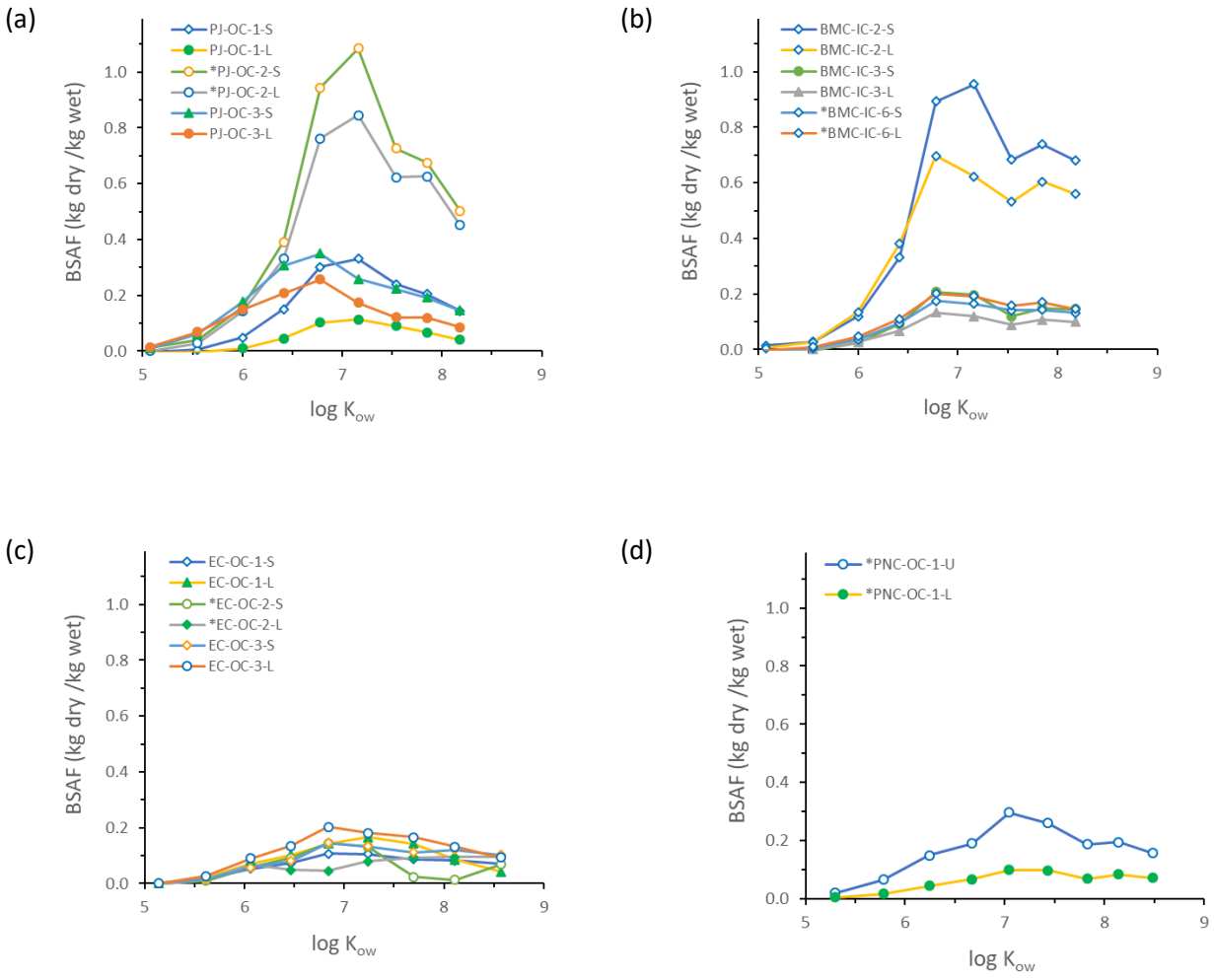

Figure 9. PCB homolog BSAFs versus log K_{ow} for: (a) Port Jersey off-channel sediment samples, (b) Buttermilk Channel in-channel samples, (c) Elizabeth Channel off-channel sediment samples, and (d) Port Newark Channel off-channel sediment samples.

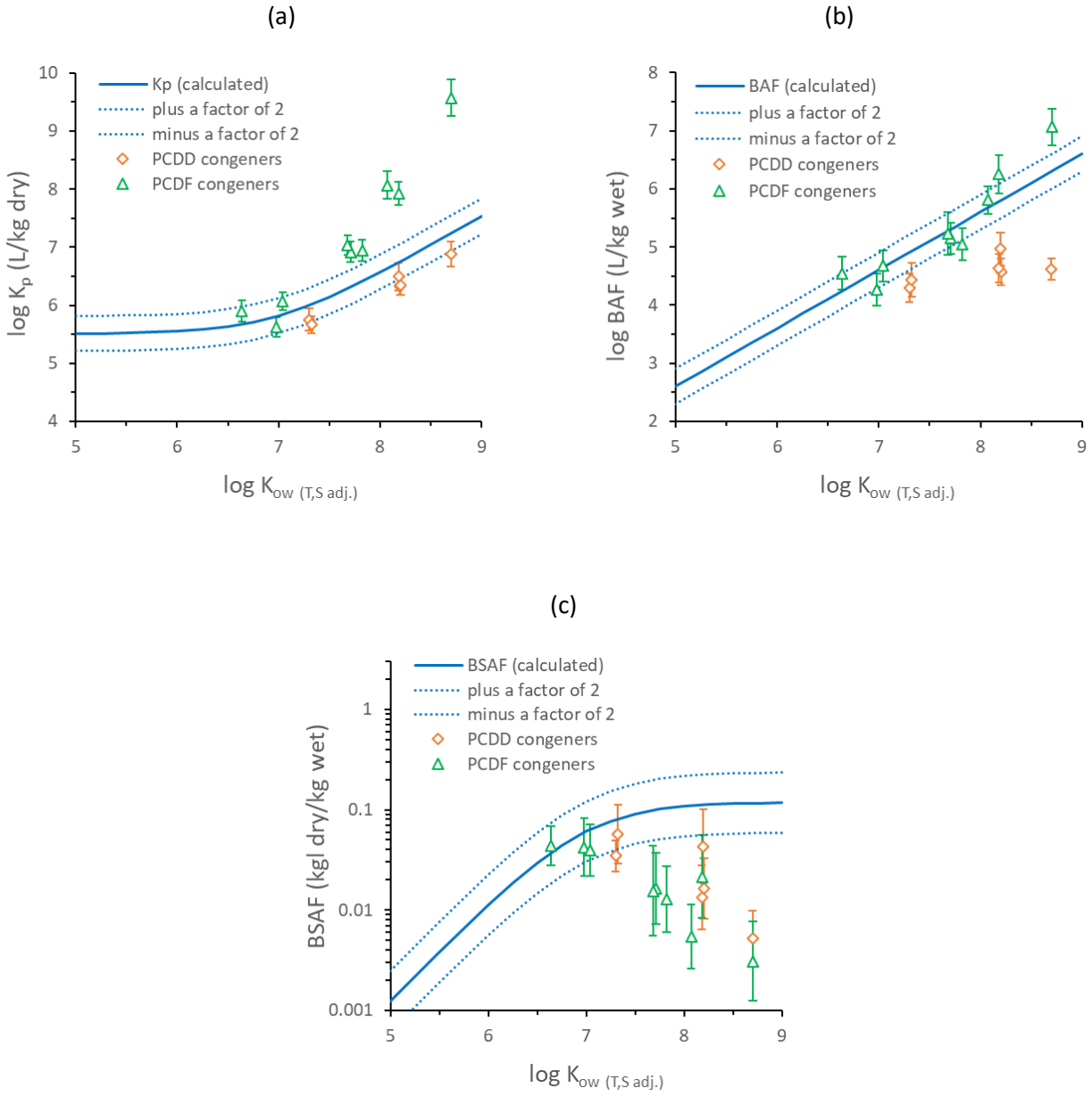

Figure 10. Comparison of calculated versus observed PCDD/F for K_p, BAF and BSAF based on Equations 11-13 and the following model coefficients that were obtained from the global fit of observed PCB congeners values for the 20 sediment samples with PCB porewater measurements: $\beta_2 = 0.253$, $\beta_1 = 1.2$ and $a_1 = 8.76 \times 10^5$. Note: observed K_ps, BAFs and BSAFs are the PCDD and PCDF congeners are plotted as geometric means $\pm$ one log standard deviation.

NY/NJ Harbor Contamination Assessment and Reduction Project

CARP II

Task 5: Develop a method (or model) for predicting bioaccumulation of sedimentary contaminants in dredged material test organisms

Appendix A. Supplemental Tables and Figures

July 2023

Table A-1. Sediment sample locations

event	Site Name	Collection Date	Sediment Depth (cm)	Channel	Position
BMC-IC-2-L	Buttermilk_Channel_2	4/16/2019	10-20	in channel	Under
BMC-IC-2-S	Buttermilk_Channel_2	4/16/2019	0-10	in channel	Over
BMC-IC-3-L	Buttermilk_Channel_3a	4/16/2019	20-30	in channel	Under
BMC-IC-3-S	Buttermilk_Channel_3a	4/16/2019	0-10	in channel	Over
BMC-IC-6-L	Buttermilk_Channel_6a	4/16/2019	20-30	in channel	Under
BMC-IC-6-S	Buttermilk_Channel_6a	4/16/2019	0-10	in channel	Over
BMC-OC-3-L	Buttermilk_Channel_3	4/16/2019	6-10	off channel	Under
BMC-OC-3-S	Buttermilk_Channel_3	4/16/2019	0-4	off channel	Over
BMC-OC-5-L	Buttermilk_Channel_5	4/16/2019	6-10	off channel	Under
BMC-OC-5-S	Buttermilk_Channel_5	4/16/2019	0-4	off channel	Over
BMC-OC-6-L	Buttermilk_Channel_6	4/16/2019	6-10	off channel	Under
BMC-OC-6-S	Buttermilk_Channel_6	4/16/2019	0-4	off channel	Over
EC-IC-1-L	Elizabeth Channel_1	5/16/2019	13-23	in channel	Under
EC-IC-1-S	Elizabeth Channel_1	5/16/2019	0-10	in channel	Over
EC-IC-2-L	Elizabeth Channel_2	5/16/2019	20-30	in channel	Under
EC-IC-2-S	Elizabeth Channel_2	5/16/2019	0-10	in channel	Over
EC-IC-3-L	Elizabeth Channel_3	5/16/2019	20-30	in channel	Under
EC-IC-3-S	Elizabeth Channel_3	5/16/2019	0-10	in channel	Over
EC-OC-1-L	Elizabeth Channel_4	5/16/2019	6-10	off channel	Under
EC-OC-1-S	Elizabeth Channel_4	5/16/2019	0-4	off channel	Over
EC-OC-2-L	Elizabeth Channel_5	5/16/2019	6-10	off channel	Under
EC-OC-2-S	Elizabeth Channel_5	5/16/2019	0-4	off channel	Over
EC-OC-3-L	Elizabeth Channel_6	5/16/2019	6-10	off channel	Under
EC-OC-3-S	Elizabeth Channel_6	5/16/2019	0-4	off channel	Over
PJ-IC-1-L	Port Jersey 1	5/7/2019	20-30	in channel	Under
PJ-IC-1-S	Port Jersey 1	5/7/2019	0-10	in channel	Over
PJ-IC-2-L	Port Jersey 2	5/7/2019	20-30	in channel	Under
PJ-IC-2-S	Port Jersey 2	5/7/2019	0-10	in channel	Over
PJ-IC-3-L	Port Jersey 3	5/7/2019	10-20	in channel	Under
PJ-IC-3-S	Port Jersey 3	5/7/2019	0-10	in channel	Over
PJ-OC-1-L	Port Jersey 4	5/7/2019	6-10	off channel	Under
PJ-OC-1-S	Port Jersey 4	5/7/2019	0-4	off channel	Over
PJ-OC-2-L	Port Jersey 5	5/7/2019	6-10	off channel	Under
PJ-OC-2-S	Port Jersey 5	5/7/2019	0-4	off channel	Over
PJ-OC-3-L	Port Jersey 6	5/7/2019	6-10	off channel	Under
PJ-OC-3-S	Port Jersey 6	5/7/2019	0-4	off channel	Over

event	Site Name	Collection Date	Sediment Depth (cm)	Channel	Position
PNC-IC-1-L	Port_Newark_7	6/13/2019	20-30	in channel	Under
PNC-IC-1-U	Port_Newark_7	6/13/2019	0-10	in channel	Over
PNC-IC-2-L	Port_Newark_8	6/13/2019	20-30	in channel	Under
PNC-IC-2-U	Port_Newark_8	6/13/2019	0-10	in channel	Over
PNC-IC-3-L	Port_Newark_9	6/13/2019	20-30	in channel	Under
PNC-IC-3-U	Port_Newark_9	6/13/2019	0-10	in channel	Over
PNC-OC-1-L	Port_Newark_10	6/13/2019	6-10	off channel	Under
PNC-OC-1-U	Port_Newark_10	6/13/2019	0-4	off channel	Over
RR-IC-1-L	Wards_Point_Bend_1	3/26/2019	20-30	in channel	Under
RR-IC-1-S	Wards_Point_Bend_1	3/26/2019	0-10	in channel	Over
RR-IC-2_L	Wards_Point_Bend_2	3/26/2019	20-30	in channel	Under
RR-IC-2-S	Wards_Point_Bend_2	3/26/2019	0-10	in channel	Over
RR-IC-3_S	Wards_Point_Bend_3	3/26/2019	0-10	in channel	Over
RR-IC-3-L	Wards_Point_Bend_3	3/26/2019	20-30	in channel	Under
RR-OC__L	Wards_Point_Bend_6	3/26/2019	6-10	off channel	Under
RR-OC__S	Wards_Point_Bend_6	3/26/2019	0-4	off channel	Over
RR-OC-1-L	Wards_Point_Bend_4	3/26/2019	6-10	off channel	Under
RR-OC-1-S	Wards_Point_Bend_4	3/26/2019	0-4	off channel	Over
RR-OC-2_S	Wards_Point_Bend_5	3/26/2019	0-4	off channel	Over
RR-OC-2-L	Wards_Point_Bend_5	3/26/2019	6-10	off channel	Under
SB-IC-1-L	South Brother_1	4/23/2019	10-20	in channel	Under
SB-IC-1-S	South Brother_1	4/23/2019	0-10	in channel	Over
SB-IC-2-L	South Brother_2	4/23/2019	10-20	in channel	Under
SB-IC-2-S	South Brother_2	4/23/2019	0-10	in channel	Over
SB-IC-3-L	South Brother_3	4/23/2019	10-20	in channel	Under
SB-IC-3-S	South Brother_3	4/23/2019	0-10	in channel	Over
SB-OC-1-L	South Brother_4	4/23/2019	6-10	off channel	Under
SB-OC-1-S	South Brother_4	4/23/2019	0-4	off channel	Over
SB-OC-2-L	South Brother_5	4/23/2019	6-10	off channel	Under
SB-OC-2-S	South Brother_5	4/23/2019	0-4	off channel	Over
SB-OC-3-L	South Brother_6	4/23/2019	6-10	off channel	Under
SB-OC-3-S	South Brother_6	4/23/2019	0-4	off channel	Over

Table A-2. Chemical parameters for PCB congeners.

Congener #	Name	Homolog	MW	TEF[a]	log K_{ow}[b]	ΔH_{OW}[c] (kJ mol^{-1})	Setschenow Constant[d]	Dihedral Angle[e]
1	2-chlorobiphenyl	1	188.66		4.46	-19.8	0.27	55.07
2	3-chlorobiphenyl	1	188.66		4.69	-20	0.27	38.51
3	4-chlorobiphenyl	1	188.66		4.69	-20	0.27	38.14
4	2,2'-dichlorobiphenyl	2	223.1		4.65	-20.7	0.29	80.49
5	2,3-dichlorobiphenyl	2	223.1		4.97	-20.9	0.29	58.03
6	2,3'-dichlorobiphenyl	2	223.1		5.06	-21	0.29	55.68
7	2,4-dichlorobiphenyl	2	223.1		5.07	-21	0.29	55.11
8	2,4'-dichlorobiphenyl	2	223.1		5.07	-21	0.29	54.86
9	2,5-dichlorobiphenyl	2	223.1		5.06	-21	0.29	55.19
10	2,6-dichlorobiphenyl	2	223.1		4.84	-20.7	0.28	85.25
11	3,3'-dichlorobiphenyl	2	223.1		5.28	-21.2	0.29	38.77
12	3,4-dichlorobiphenyl	2	223.1		5.22	-21.1	0.29	38.01
13	3,4'-dichlorobiphenyl	2	223.1		5.29	-21.2	0.29	38.28
14	3,5-dichlorobiphenyl	2	223.1		5.28	-21.2	0.29	38.42
15	4,4'-dichlorobiphenyl	2	223.1		5.3	-21.2	0.29	37.53
16	2,2',3-trichlorobiphenyl	3	257.54		5.16	-21.6	0.3	84.72
17	2,2',4-trichlorobiphenyl	3	257.54		5.25	-21.8	0.3	80.10
18	2,2',5-trichlorobiphenyl	3	257.54		5.24	-21.9	0.3	80.02
19	2,2',6-trichlorobiphenyl	3	257.54		5.02	-21.5	0.3	89.27
20	2,3,3'-trichlorobiphenyl	3	257.54		5.57	-22	0.3	58.63
21	2,3,4-trichlorobiphenyl	3	257.54		5.51	-21.9	0.3	58.17
22	2,3,4'-trichlorobiphenyl	3	257.54		5.58	-22	0.3	57.62
23	2,3,5-trichlorobiphenyl	3	257.54		5.57	-22.1	0.3	57.97
24	2,3,6-trichlorobiphenyl	3	257.54		5.35	-21.7	0.3	87.83
25	2,3',4-trichlorobiphenyl	3	257.54		5.67	-22.2	0.3	55.47

Congener #	Name	Homolog	MW	TEF[a]	log K_{ow}[b]	ΔH_{OW}[c] (kJ mol^{-1})	Setschenow Constant[d]	Dihedral Angle[e]
26	2,3',5-trichlorobiphenyl	3	257.54		5.66	-22.2	0.3	55.48
27	2,3',6-trichlorobiphenyl	3	257.54		5.44	-21.9	0.3	89.54
28	2,4,4'-trichlorobiphenyl	3	257.54		5.67	-22.2	0.3	54.69
29	2,4,5-trichlorobiphenyl	3	257.54		5.6	-22.1	0.3	54.72
30	2,4,6-trichlorobiphenyl	3	257.54		5.44	-21.9	0.3	84.58
31	2,4',5-trichlorobiphenyl	3	257.54		5.67	-22.2	0.3	54.78
32	2,4',6-trichlorobiphenyl	3	257.54		5.44	-21.9	0.3	82.93
33	2',3,4-trichlorobiphenyl	3	257.54		5.6	-22	0.3	54.99
34	2',3,5-trichlorobiphenyl	3	257.54		5.66	-22.2	0.3	55.74
35	3,3',4-trichlorobiphenyl	3	257.54		5.82	-22.3	0.3	38.33
36	3,3',5-trichlorobiphenyl	3	257.54		5.88	-22.4	0.3	38.73
37	3,4,4'-trichlorobiphenyl	3	257.54		5.83	-22.3	0.3	37.73
38	3,4,5-trichlorobiphenyl	3	257.54		5.76	-22.2	0.3	37.87
39	3,4',5-trichlorobiphenyl	3	257.54		5.89	-22.4	0.3	38.25
40	2,2',3,3'-tetrachlorobiphenyl	4	291.98		5.66	-22.8	0.31	86.62
41	2,2' ,3,4-tetrachlorobiphenyl	4	291.98		5.69	-22.8	0.31	81.64
42	2,2',3,4'-tetrachlorobiphenyl	4	291.98		5.76	-22.9	0.31	82.13
43	2,2',3,5-tetrachlorobiphenyl	4	291.98		5.75	-22.9	0.31	82.39
44	2,2',3,5'-tetrachlorobiphenyl	4	291.98		5.75	-23	0.31	81.36
45	2,2',3,6-tetrachlorobiphenyl	4	291.98		5.53	-22.5	0.31	89.40
46	2,2',3,6'-tetrachlorobiphenyl	4	291.98		5.53	-22.5	0.31	88.89
47	2,2',4,4'-tetrachlorobiphenyl	4	291.98		5.85	-23	0.31	79.76
48	2,2',4,5-tetrachlorobiphenyl	4	291.98		5.78	-23	0.31	79.13
49	2,2',4,5'-tetrachlorobiphenyl	4	291.98		5.85	-23.1	0.31	79.65
50	2,2',4,6-tetrachlorobiphenyl	4	291.98		5.63	-22.7	0.31	89.23
51	2,2',4,6'-tetrachlorobiphenyl	4	291.98		5.63	-22.7	0.31	89.25

Congener #	Name	Homolog	MW	TEF[a]	log K_{ow}[b]	ΔH_{OW}[c] (kJ mol^{-1})	Setschenow Constant[d]	Dihedral Angle[e]
52	2,2',5,5'-tetrachlorobiphenyl	4	291.98		5.84	-23.1	0.31	79.85
53	2,2',5,6'-tetrachlorobiphenyl	4	291.98		5.62	-22.7	0.31	89.44
54	2,2',6,6'-tetrachlorobiphenyl	4	291.98		5.21	-22.2	0.31	89.94
55	2,3,3',4-tetrachloroblphenyl	4	291.98		6.11	-23.1	0.31	58.77
56	2,3,3',4'-tetrachlorobiphenyl	4	291.98		6.11	-23.1	0.31	57.89
57	2,3,3',5-tetrachlorobiphenyl	4	291.98		6.17	-23.2	0.31	58.47
58	2,3,3',5'-tetrachlorobiphenyl	4	291.98		6.17	-23.2	0.31	58.75
59	2,3,3',6-tetrachlorobiphenyl	4	291.98		5.95	-22.9	0.31	89.86
60	2,3,4,4'-tetrachlorobiphenyl	4	291.98		6.11	-23.1	0.31	57.80
61	2,3,4,5-tetrachlorobiphenyl	4	291.98		6.04	-22.9	0.31	57.98
62	2,3,4,6-tetrachlorobiphenyl	4	291.98		5.89	-22.8	0.31	88.94
63	2,3,4',5-tetrachlorobiphenyl	4	291.98		6.17	-23.2	0.31	57.58
64	2,3,4',6-tetrachlorobiphenyl	4	291.98		5.95	-23	0.31	88.75
65	2,3,5,6-tetrachlorobiphenyl	4	291.98		5.86	-22.8	0.31	89.74
66	2,3',4,4'-tetrachlorobiphenyl	4	291.98		6.2	-23.2	0.31	52.80
67	2,3',4,5-tetrachlorobiphenyl	4	291.98		6.2	-23.3	0.31	55.04
68	2,3',4,5'-tetrachlorobiphenyl	4	291.98		6.26	-23.4	0.31	55.60
69	2,3',4,6-tetrachlorobiphenyl	4	291.98		6.04	-23.1	0.31	89.08
70	2,3',4',5-tetrachlorobiphenyl	4	291.98		6.2	-23.2	0.32	54.89
71	2,3' ,4' ,6-tetrachlorobiphenyl	4	291.98		5.98	-22.9	0.31	89.10
72	2,3',5,5'-tetrachlorobiphenyl	4	291.98		6.26	-23.4	0.31	55.79
73	2,3',5',6-tetrachlorobiphenyl	4	291.98		6.04	-23.1	0.31	89.96
74	2,4,4',5-tetrachlorobiphenyl	4	291.98		6.2	-23.2	0.31	54.32
75	2,4,4',6-tetrachlorobiphenyl	4	291.98		6.05	-23.1	0.31	82.60
76	2',3,4,5-tetrachlorobiphenyl	4	291.98		6.13	-23.1	0.31	54.96
77	3,3',4,4'-tetrachlorobiphenyl	4	291.98	0.0001	6.36	-23.3	0.32	37.89

Congener #	Name	Homolog	MW	TEF[a]	log K_{ow}[b]	ΔH_{OW}[c] (kJ mol^{-1})	Setschenow Constant[d]	Dihedral Angle[e]
78	3,3',4,5-tetrachlorobiphenyl	4	291.98		6.35	-23.3	0.32	38.18
79	3,3',4,5'-tetrachlorobiphenyl	4	291.98		6.42	-23.5	0.32	38.35
80	3,3',5,5'-tetrachlorobiphenyl	4	291.98		6.48	-23.7	0.32	39.09
81	3,4,4',5-tetrachlorobiphenyl	4	291.98	0.0003	6.36	-23.3	0.32	37.67
82	2,2',3,3',4-pentachlorobiphenyl	5	326.42		6.2	-23.8	0.33	87.06
83	2,2',3,3',5-pentachlorobiphenyl	5	326.42		6.26	-23.9	0.33	83.47
84	2,2',3,3',6-pentachlorobiphenyl	5	326.42		6.04	-23.5	0.33	89.27
85	2,2',3,4,4'-pentachlorobiphenyl	5	326.42		6.3	-24	0.33	82.82
86	2,2',3,4,5-pentachlorobiphenyl	5	326.42		6.23	-23.8	0.33	81.94
87	2,2',3,4,5'-pentachlorobiphenyl	5	326.42		6.29	-24	0.33	81.73
88	2,2',3,4,6-pentachlorobiphenyl	5	326.42		6.07	-23.6	0.33	89.12
89	2,2',3,4,6'-pentachlorobiphenyl	5	326.42		6.07	-23.6	0.33	88.99
90	2,2',3,4',5-pentachlorobiphenyl	5	326.42		6.36	-24.1	0.33	82.14
91	2,2',3,4',6-pentachlorobiphenyl	5	326.42		6.13	-23.7	0.33	88.96
92	2,2',3,5,5'-pentachlorobiphenyl	5	326.42		6.35	-24.2	0.33	81.53
93	2,2',3,5,6-pentachlorobiphenyl	5	326.42		6.04	-23.5	0.33	89.20
94	2,2',3,5,6'-pentachlorobiphenyl	5	326.42		6.13	-23.7	0.33	89.31
95	2,2',3,5',6-pentachlorobiphenyl	5	326.42		6.13	-23.8	0.33	89.08
96	2,2',3,6,6'-pentachlorobiphenyl	5	326.42		5.71	-23.2	0.33	89.85
97	2,2',3',4,5-pentachlorobiphenyl	5	326.42		6.29	-24	0.33	80.77
98	2,2',3',4,6-pentachlorobiphenyl	5	326.42		6.13	-23.8	0.33	89.26
99	2,2',4,4',5-pentachlorobiphenyl	5	326.42		6.39	-24.2	0.33	78.77
100	2,2',4,4',6-pentachlorobiphenyl	5	326.42		6.23	-23.9	0.33	89.20
101	2,2',4,5.5'-pentachlorobiphenyl	5	326.42		6.38	-24.1	0.33	79.10
102	2,2',4,5,6'-pentachlorobiphenyl	5	326.42		6.16	-23.8	0.33	89.38
103	2,2',4,5',6-pentachlorobiphenyl	5	326.42		6.22	-24	0.33	89.35

Congener #	Name	Homolog	MW	TEF[a]	log K_{ow}[b]	ΔH_{OW}[c] (kJ mol^{-1})	Setschenow Constant[d]	Dihedral Angle[e]
104	2,2',4,6,6'-pentachlorobiphenyl	5	326.42		5.81	-23.4	0.33	89.99
105	2,3,3',4,4'-pentachlorobiphenyl	5	326.42	0.00003	6.65	-24.1	0.33	58.03
106	2,3,3',4,5-pentachlorobiphenyl	5	326.42		6.64	-24.1	0.33	58.46
107	2,3,3',4',5-pentachlorobiphenyl	5	326.42		6.71	-24.3	0.33	57.82
108	2,3,3',4,5'-pentachlorobiphenyl	5	326.42		6.71	-24.3	0.33	58.89
109	2,3,3',4,6-pentachlorobiphenyl	5	326.42		6.48	-24	0.33	89.89
110	2,3,3',4',6-pentachlorobiphenyl	5	326.42		6.48	-24	0.33	89.61
111	2,3,3',5,5'-pentachlorobiphenyl	5	326.42		6.76	-24.5	0.33	58.85
112	2,3,3',5,6-pentachlorobiphenyl	5	326.42		6.45	-24	0.33	89.34
113	2,3,3',5',6-pentachlorobiphenyl	5	326.42		6.54	-24.2	0.33	89.90
114	2,3,4,4',5-pentachlorobiphenyl	5	326.42	0.00003	6.65	-24.1	0.33	57.58
115	2,3,4,4',6-pentachlorobiphenyl	5	326.42		6.49	-24	0.33	83.08
116	2,3,4,5,6-pentachlorobiphenyl	5	326.42		6.33	-23.7	0.33	89.00
117	2,3,4',5,6-pentachlorobiphenyl	5	326.42		6.46	-24	0.33	89.77
118	2,3',4,4',5-pentachlorobiphenyl	5	326.42	0.00003	6.74	-24.3	0.33	54.41
119	2,3',4,4',6-pentachlorobiphenyl	5	326.42		6.58	-24.2	0.33	88.26
120	2,3',4,5,5'-pentachlorobiphenyl	5	326.42		6.79	-24.5	0.33	55.37
121	2,3',4,5',6-pentachlorobiphenyl	5	326.42		6.64	-24.3	0.33	89.15
122	2',3,3',4,5-pentachlorobiphenyl	5	326.42		6.64	-24.1	0.33	57.93
123	2',3,4,4',5-pentachlorobiphenyl	5	326.42	0.00003	6.74	-24.3	0.33	54.82
124	2',3,4,5,5'-pentachlorobiphenyl	5	326.42		6.73	-24.3	0.33	55.05
125	2',3,4,5,6'-pentachlorobiphenyl	5	326.42		6.51	-24	0.33	89.97
126	3,3',4,4',5-pentachlorobiphenyl	5	326.42	0.1	6.89	-24.4	0.33	37.71
127	3,3',4,5,5'-pentachlorobiphenyl	5	326.42		6.95	-24.5	0.33	38.48
128	2,2',3,3',4,4'-hexachlorobiphenyl	6	360.86		6.74	-24.9	0.34	89.02
129	2,2',3,3',4,5-hexachlorobiphenyl	6	360.86		6.73	-24.9	0.34	83.18

Congener #	Name	Homolog	MW	TEF[a]	log K_{ow}[b]	ΔH_{OW}[c] (kJ mol^{-1})	Setschenow Constant[d]	Dihedral Angle[e]
130	2,2',3,3',4,5'-hexachlorobiphenyl	6	360.86		6.8	-25	0.34	83.50
131	2,2',3,3',4,6-hexachlorobiphenyl	6	360.86		6.58	-24.6	0.34	89.05
132	2,2',3,3',4,6'-hexachlorobiphenyl	6	360.86		6.58	-24.6	0.34	89.50
133	2,2',3,3',5,5'-hexachlorobiphenyl	6	360.86		6.86	-25.2	0.34	82.65
134	2,2',3,3',5,6-hexachlorobiphenyl	6	360.86		6.55	-24.6	0.34	89.05
135	2,2' ,3,3' ,5,6'-hexachlorobiphenyl	6	360.86		6.64	-24.8	0.34	89.37
136	2,2',3,3',6,6'-hexachlorobiphenyl	6	360.86		6.22	-24.3	0.34	89.92
137	2,2',3,4,4',5-hexachlorobiphenyl	6	360.86		6.83	-25	0.34	81.76
138	2,2',3,4,4',5'-hexachlorobiphenyl	6	360.86		6.83	-25	0.34	81.11
139	2,2',3,4,4',6-hexachlorobiphenyl	6	360.86		6.67	-24.8	0.34	89.70
140	2,2',3,4,4',6'-hexachlorobiphenyl	6	360.86		6.67	-24.8	0.34	89.18
141	2,2',3,4,5,5'-hexachlorobiphenyl	6	360.86		6.82	-25.1	0.34	81.12
142	2,2',3,4,5,6-hexachlorobiphenyl	6	360.86		6.51	-24.4	0.34	89.30
143	2,2',3,4,5,6'-hexachlorobiphenyl	6	360.86		6.6	-24.6	0.34	89.28
144	2,2',3,4,5',6-hexachlorobiphenyl	6	360.86		6.67	-24.8	0.34	89.51
145	2,2',3,4,6,6'-hexachlorobiphenyl	6	360.86		6.25	-24.3	0.34	89.69
146	2,2',3,4',5,5'-hexachlorobiphenyl	6	360.86		6.89	-25.2	0.34	80.96
147	2,2',3,4',5,6-hexachlorobiphenyl	6	360.86		6.64	-24.8	0.34	89.22
148	2,2',3,4',5,6'-hexachlorobiphenyl	6	360.86		6.73	-25	0.34	89.30
149	2,2',3,4',5',6-hexachlorobiphenyl	6	360.86		6.67	-24.8	0.34	89.43
150	2,2',3,4',6,6'-hexachlorobiphenyl	6	360.86		6.32	-24.5	0.34	89.77
151	2,2' ,3,S,S' ,6-hexachlorobiphenyl	6	360.86		6.64	-24.8	0.34	89.28
152	2,2',3,5,6,6'-hexachlorobiphenyl	6	360.86		6.22	-24.3	0.34	89.81
153	2,2',4,4',5,5'-hexachlorobiphenyl	6	360.86		6.92	-25.2	0.34	78.49
154	2,2',4,4',5,6-hexachlorobiphenyl	6	360.86		6.76	-25	0.34	89.40
155	2,2',4,4',6,6'-hexachlorobiphenyl	6	360.86		6.41	-24.6	0.34	89.98

Congener #	Name	Homolog	MW	TEF[a]	log K_{ow}[b]	ΔH_{OW}[c] (kJ mol^{-1})	Setschenow Constant[d]	Dihedral Angle[e]
156	2,3,3',4,4',5-hexachlorobiphenyl	6	360.86	0.00003	7.18	-25.2	0.34	57.81
157	2,3,3',4,4',5'-hexachlorobiphenyl	6	360.86	0.00003	7.18	-25.2	0.34	58.05
158	2,3,3',4,4',6-hexachlorobiphenyl	6	360.86		7.02	-25	0.34	89.85
159	2,3,3',4,5,5'-hexachlorobiphenyl	6	360.86		7.24	-25.4	0.34	58.84
160	2,3,4,4',5,6-hexachlorobiphenyl	6	360.86		6.93	-24.9	0.34	89.91
161	2,3,3',4,5',6-hexachlorobiphenyl	6	360.86		7.08	-25.2	0.34	89.99
162	2,3,3',4',5,5'-hexachlorobiphenyl	6	360.86		7.24	-25.4	0.34	58.00
163	2,3,3' ,4' ,5,6-hexachlorobiphenyl	6	360.86		6.99	-25	0.34	88.84
164	2,3,3',4',5',6-hexachlorobiphenyl	6	360.86		7.02	-25.1	0.34	88.92
165	2,3,3',5,5',6-hexachlorobiphenyl	6	360.86		7.05	-25.2	0.34	89.63
166	2,3,4,4',5,6-hexachlorobiphenyl	6	360.86		6.93	-24.9	0.34	89.20
167	2,3',4,4',5,5'-hexachlorobiphenyl	6	360.86	0.00003	7.27	-25.3	0.34	54.59
168	2,3',4,4',5',6-hexachlorobiphenyl	6	360.86		7.11	-25.2	0.34	78.50
169	3,3',4,4',5,5'-hexachlorobiphenyl	6	360.86	0.03	7.42	-25.4	0.34	37.80
170	2,2',3,3',4,4',5-heptachlorobiphenyl	7	395.3		7.27	-25.9	0.35	83.11
171	2,2',3,3',4,4',6-heptachlorobiphenyl	7	395.3		7.11	-25.7	0.36	89.32
172	2,2',3,3',4,5,5'-heptachlorobiphenyl	7	395.3		7.33	-26.1	0.35	82.32
173	2,2',3,3',4,5,6-heptachlorobiphenyl	7	395.3		7.02	-25.5	0.35	88.93
174	2,2',3,3',4,5,6'-heptachlorobiphenyl	7	395.3		7.11	-25.7	0.35	89.68
175	2,2',3,3',4,5',6-heptachlorobiphenyl	7	395.3		7.17	-25.8	0.35	89.07
176	2,2',3,3',4,6,6'-heptachlorobiphenyl	7	395.3		6.76	-25.3	0.35	89.96
177	2,2',3,3',4',5,6-heptachlorobiphenyl	7	395.3		7.08	-25.6	0.36	89.11
178	2,2',3,3',5,5',6-heptachlorobiphenyl	7	395.3		7.14	-25.8	0.35	89.15
179	2,2',3,3',5,6,6'-heptachlorobiphenyl	7	395.3		6.73	-25.3	0.35	89.71
180	2,2',3,4,4',5,5'-heptachlorobiphenyl	7	395.3		7.36	-26.1	0.36	80.82
181	2,2',3,4,4',5,6-heptachlorobiphenyl	7	395.3		7.11	-25.6	0.36	89.35

Congener #	Name	Homolog	MW	TEF[a]	log K_{ow}[b]	ΔH_{OW}[c] (kJ mol^{-1})	Setschenow Constant[d]	Dihedral Angle[e]
182	2,2',3,4,4',5,6'-heptachlorobiphenyl	7	395.3		7.2	-25.9	0.36	89.46
183	2,2',3,4,4',5',6-heptachlorobiphenyl	7	395.3		7.2	-25.9	0.36	89.61
184	2,2',3,4,4',6,6'-heptachlorobiphenyl	7	395.3		6.85	-25.5	0.36	89.84
185	2,2',3,4,5,5',6-heptachlorobiphenyl	7	395.3		7.11	-25.7	0.35	89.44
186	2,2',3,4,5,6,6'-heptachlorobiphenyl	7	395.3		6.69	-25.2	0.36	89.93
187	2,2',3,4',5,5',6-heptachlorobiphenyl	7	395.3		7.17	-25.8	0.35	89.41
188	2,2',3,4',5,6,6'-heptachlorobiphenyl	7	395.3		6.82	-25.5	0.36	89.98
189	2,3,3',4,4',5,5'-heptachlorobiphenyl	7	395.3	0.00003	7.71	-26.2	0.36	58.00
190	2,3,3',4,4',5,6-heptachlorobiphenyl	7	395.3		7.46	-25.9	0.35	89.61
191	2,3,3',4,4',5',6-heptachlorobiphenyl	7	395.3		7.55	-26.1	0.35	87.09
192	2,3,3',4,5,5',6-heptachlorobiphenyl	7	395.3		7.52	-26.1	0.35	89.94
193	2,3,3',4',5,5',6-heptachlorobiphenyl	7	395.3		7.52	-26.1	0.35	89.28
194	2,2',3,3',4,4',5,5'-octachlorobiphenyl	8	429.74		7.8	-27	0.37	83.57
195	2,2',3,3',4,4',5,6-octachlorobiphenyl	8	429.74		7.56	-26.5	0.37	88.98
196	2,2',3,3',4,4',5',6-octachlorobiphenyl	8	429.74		7.65	-26.7	0.37	89.66
197	2,2',3,3',4,4',6,6'-octachlorobiphenyl	8	429.74		7.3	-26.4	0.37	90.00
198	2,2',3,3',4,5,5',6-octachlorobiphenyl	8	429.74		7.62	-26.7	0.37	89.07
199	2,2',3,3',4,5,6,6'-octachlorobiphenyl	8	429.74		7.62	-26.7	0.37	89.21
200	2,2',3,3',4,5',6,6'-octachlorobiphenyl	8	429.74		7.2	-26.2	0.37	89.71
201	2,2',3,3',4,5',6,6'-octachlorobiphenyl	8	429.74		7.27	-26.4	0.37	89.81
202	2,2',3,3',5,5',6,6'-octachlorobiphenyl	8	429.74		7.24	-26.4	0.37	89.97
203	2,2',3,4,4',5,5',6-octachlorobiphenyl	8	429.74		7.65	-26.7	0.37	89.47
204	2,2',3,4,4',5,6,6'-octachlorobiphenyl	8	429.74		7.3	-26.4	0.37	89.99
205	2,3,3',4,4',5,5',6-octachlorobiphenyl	8	429.74		8	-27	0.37	89.98
206	2,2',3,3',{4',5,5',6-nonachlorobiphenyl	9	464.18		8.09	-27.6	0.38	89.18
207	2,2',3,3',4,4',5,6,6'-nonachlorobiphenyl	9	464.18		7.74	-27.3	0.38	89.76

Congener #	Name	Homolog	MW	TEF[a]	log K_{ow}[b]	ΔH_{OW}[c] (kJ mol^{-1})	Setschenow Constant[d]	Dihedral Angle[e]
208	2,2',3,3',4,5,5',6,6'-nonachlorobiphenyl	9	464.18		7.71	-27.3	0.38	89.99
209	2,2',3,3',4,4',5,5',6,6'-decachlorobiphenyl	10	498.62		8.18	-28.1	0.4	90.00

[a] Toxic Equivalent Factors (TEF) from U.S. Environmental Protection Agency (2010).

[b] Log K_{ow} values from Hawker and Connell (1988).

[c] ΔH_{ow} values from Greene et al. (2013).

[d] Setschenow constants (K^{salt}) from the UFZ-LSER database v 3.2.1 (Ulrich et al. 2017).

[e] Dihedral angles from Greene et al. (2013).

Table A-3. Chemical parameters for PCDD/F congeners.

Congener #	Name	Homolog	MW	TEF[a]	log K_{ow}[b]	TSA[c]	ΔH_{OW}[d] (kJ mol^{-1})	Setschenow Constant[e]
1	2,3,7,8-TCDD	4	321.8	1	7.05	297	-24.98	0.31
2	1,2,3,7,8-PECDD	5	356.25	1	7.06	309	-25.74	0.33
3	1,2,3,4,7,8-HXCDD	6	390.7	0.1	7.93	321	-26.51	0.34
4	1,2,3,6,7,8-HXCDD	6	390.7	0.1	7.93	321	-26.51	0.34
5	1,2,3,7,8,9-HXCDD	6	390.7	0.1	7.91	321	-26.51	0.34
6	1,2,3,4,6,7,8-HPCDD	7	425.15	0.01	8.42	338	-27.59	0.35
7	OCDD	8	459.6	0.0003	8.85	350[f]	-28.35	0.35
8	2,3,7,8-TCDF	4	305.8	0.1	6.41	247.7	-21.84	0.29
9	1,2,3,7,8-PECDF	5	340.25	0.03	6.74	261.9[g]	-22.75	0.31
10	2,3,4,7,8-PECDF	5	340.25	0.3	6.8	262.7	-22.80	0.31
11	1,2,3,6,7,8-HXCDF	6	374.7	0.1	7.56	274.9	-23.57	0.34
12	1,2,3,4,7,8-HXCDF	6	374.7	0.1	7.46	276.4	-23.67	0.32
13	1,2,3,7,8,9-HXCDF	6	374.7	0.1	7.44	275.0[g]	-23.58	
14	2,3,4,6,7,8-HXCDF	6	374.7	0.1	7.43	275.0[g]	-23.58	0.32
15	1,2,3,4,6,7,8-HPCDF	7	409.15	0.01	7.81	289.6	-24.51	0.34
16	1,2,3,4,7,8,9-HPCDF	7	409.15	0.01	7.92	286	-24.28	0.34
17	OCDF	8	443.6	0.0003	8.43	300.4	-25.20	0.35

(a) Toxic Equivalent Factors (TEF) from U.S. Environmental Protection Agency (2010).

(b) Log K_{ow} values from Sacan et al. (2005).

(c) Total surface area (TSA) for PCDDs and PCDFs are from Friesen and Webster (1990) and Dunn III et al. (1986), respectively— as reported in Mackay et al. (1991).

(d) ΔH_{ow} values estimated from ΔH_{ow} relationship in Greene et al. (2013): $\Delta H_{ow} = -0.0636 \times TSA_{cavity} - 6.09$.

(e) Setschenow constants (K^{salt}) from the UFZ-LSER database v 3.2.1 (Ulrich et al. 2017).

(f) TSA for OCDD estimated from TSA-molecular weight regression equation: $TSA = 0.3919\,MW + 169.9$; $R^2 = 0.9918$ that was developed from TSA values given for the other PCDD congeners.

(g) TSA for 1,2,3,7,8-PECDF, 1,2,3,7,8,9-HXCDF and 2,3,4,6,7,8-HXCDF estimated from TSA-molecular weight regression equation: $TSA = 0.3783\,MW + 133.21$; $R^2 = 0.994$ that was developed from TSA values given for the other PCDF congeners.

Table A-4. Listing of PCB co-eluting congeners.

PCB #	Co-elutes
1	1
2	2
3	3
4	4, 10
5	5, 8
6	6
7	7, 9
11	11
12	12, 13
14	14
15	15
16	16, 32
17	17
18	18, 30
19	19
20	20, 21, 28, 31, 33
22	22
23	23, 34
24	24, 27
25	25
26	26, 29
35	35
36	36
37	37
38	38
39	39

PCB #	Co-elutes
40	40, 41, 71, 72
42	42
43	43, 52
44	44, 47, 48, 59, 62, 65, 75
45	45, 51
46	46
49	49, 69, 73
50	50, 53
54	54
55	55
56	56, 60
57	57
58	58
61	61, 70, 74, 76
63	63
64	64, 68
66	66, 80
67	67
77	77
78	78
79	79
81	81
82	82
83	83, 99, 109

PCB #	Co-elutes
84	84, 92
85	85, 86, 87, 97, 107, 108, 110, 111, 115, 116, 117, 119, 120, 124, 125
88	88, 91, 93, 95, 98, 100, 102
89	89
90	90, 101, 113
94	94
96	96
103	103
104	104
105	105
106	106, 118
112	112
114	114
121	121
122	122
123	123
126	126
127	127
128	128, 166
129	129, 138, 158, 160, 163, 164
130	130

PCB #	Co-elutes
131	131, 133, 142
132	132, 153, 168
134	134, 143
135	135, 144, 151, 154
136	136
137	137
139	139, 140, 147, 149
141	141
145	145
146	146, 161, 165
148	148
150	150
152	152
155	155
156	156, 157
159	159
162	162
167	167
169	169
170	170, 190
171	171, 173
172	172, 192
174	174, 181
175	175
176	176

PCB #	Co-elutes
177	177
178	178
179	179
180	180, 193
182	182, 187
183	183, 185
184	184
186	186
188	188
189	189
191	191
194	194
195	195
196	196, 203
197	197, 200
198	198, 199
201	201
202	202
204	204
205	205
206	206
207	207
208	208
209	209

Notes:

Co-eluting congeners were assigned to the lowest congener number.

Chemical and toxicity parameters (TEF, log K_{ow}, ΔH_{OW}, K^{salt}) were computed as averages of the co-eluting congeners.

In addition to co-eluting congeners reported by the laboratories, final adjustments of co-eluting congeners were made to account for overlapping co-elutes in the sediment/tissue dataset (SGS AXYS) and porewater dataset (University of Rhode Island):

28 –-> 20 (20+21+28+31+33)
41 –-> 40 (40+41+71+72)
47,59 –-> 44 (44+47+48+59+62+65+75)
69 –-> 49 (49+69+73)
86,87,107,110 –-> 85 (85+86+87+97+107+108+110+111+115+116+117+119+120+124+125)
93 –-> 88 (88+91+93+95+98+100+102)
138,163 –-> 129 (129+138+158+160+163+164)
147 –-> 139 (139+140+147+149)

Combination of the sediment/tissue dataset (SGS AXYS) and porewater dataset (U. of Rhode Island) are all within homolog groups and so the combination does not affect homolog concentrations.

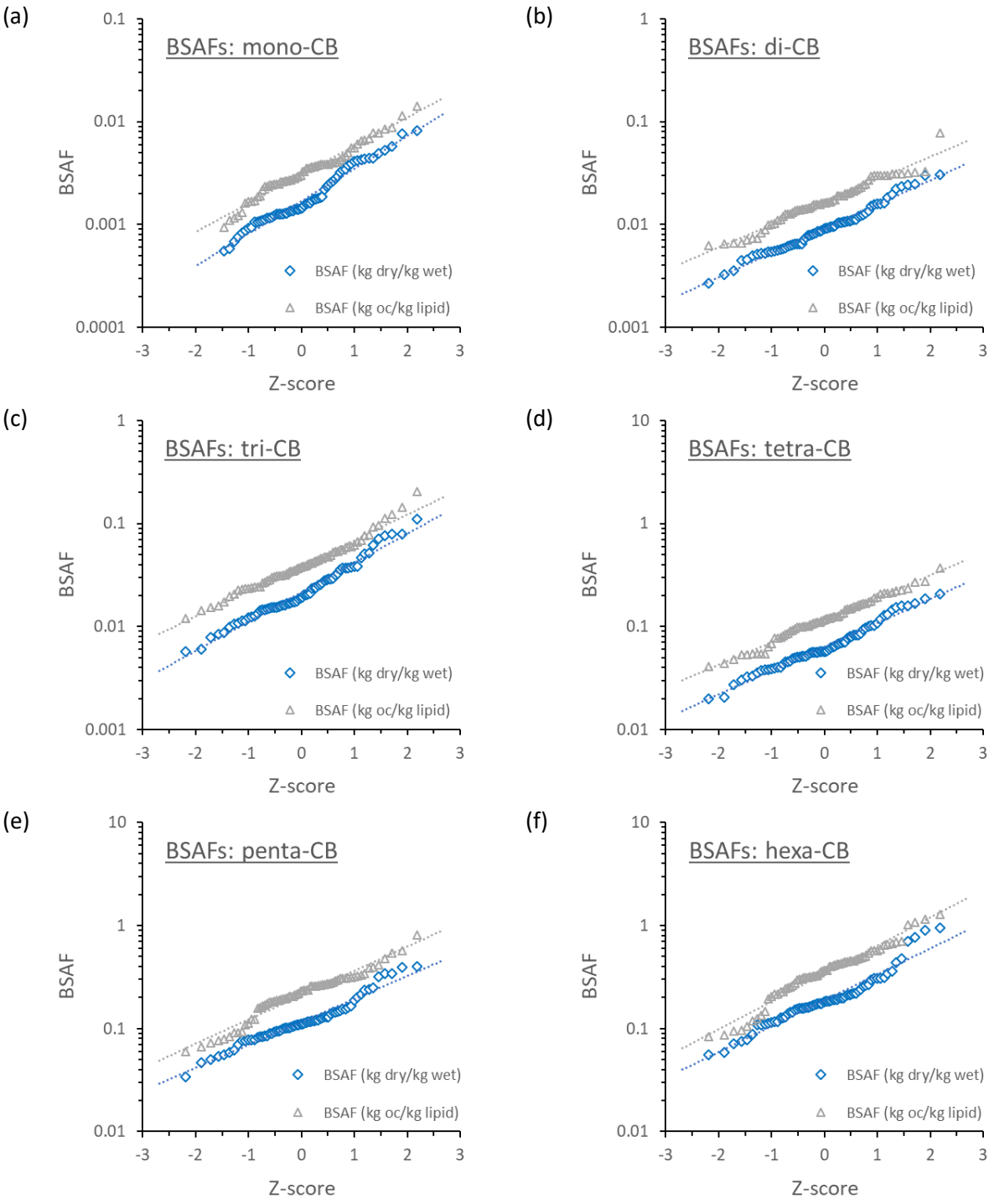

Figure A-1. Comparison of lipid:organic normalization of 28-day BSAF and non-normalized 28-day BSAF probability distributions for PCB homologs. Note: there are changes in the scale of the y-axis for mono-CB, di-CB and tri-CB.

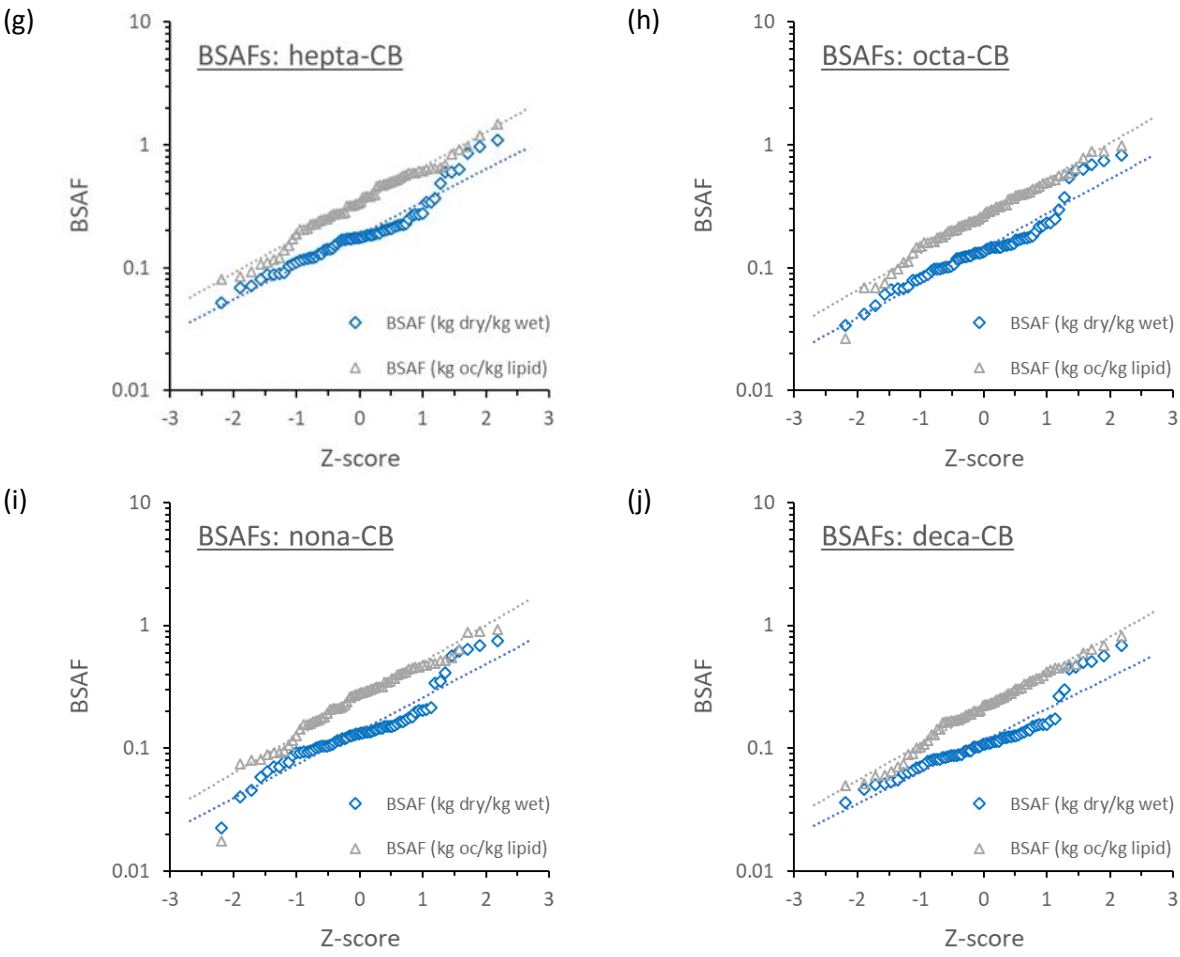

Figure A-1 (continued). Comparison of lipid:organic normalization of 28-day BSAF and non-normalized 28-day BSAF probability distributions for PCB homologs.

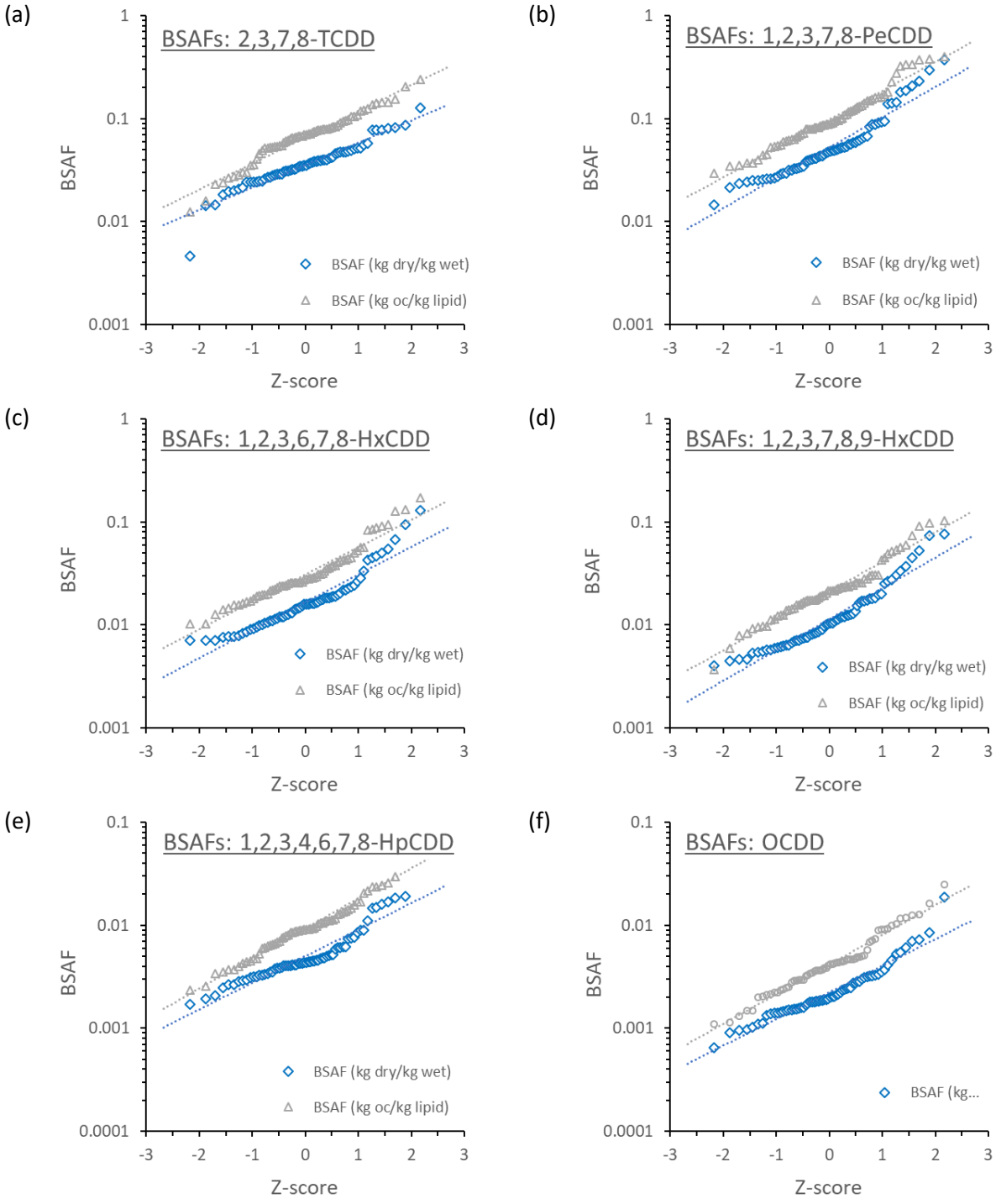

Figure A-2. Comparison of lipid:organic normalization of 28-day BSAF and non-normalized 28-day BSAF probability distributions for PCDD congeners.

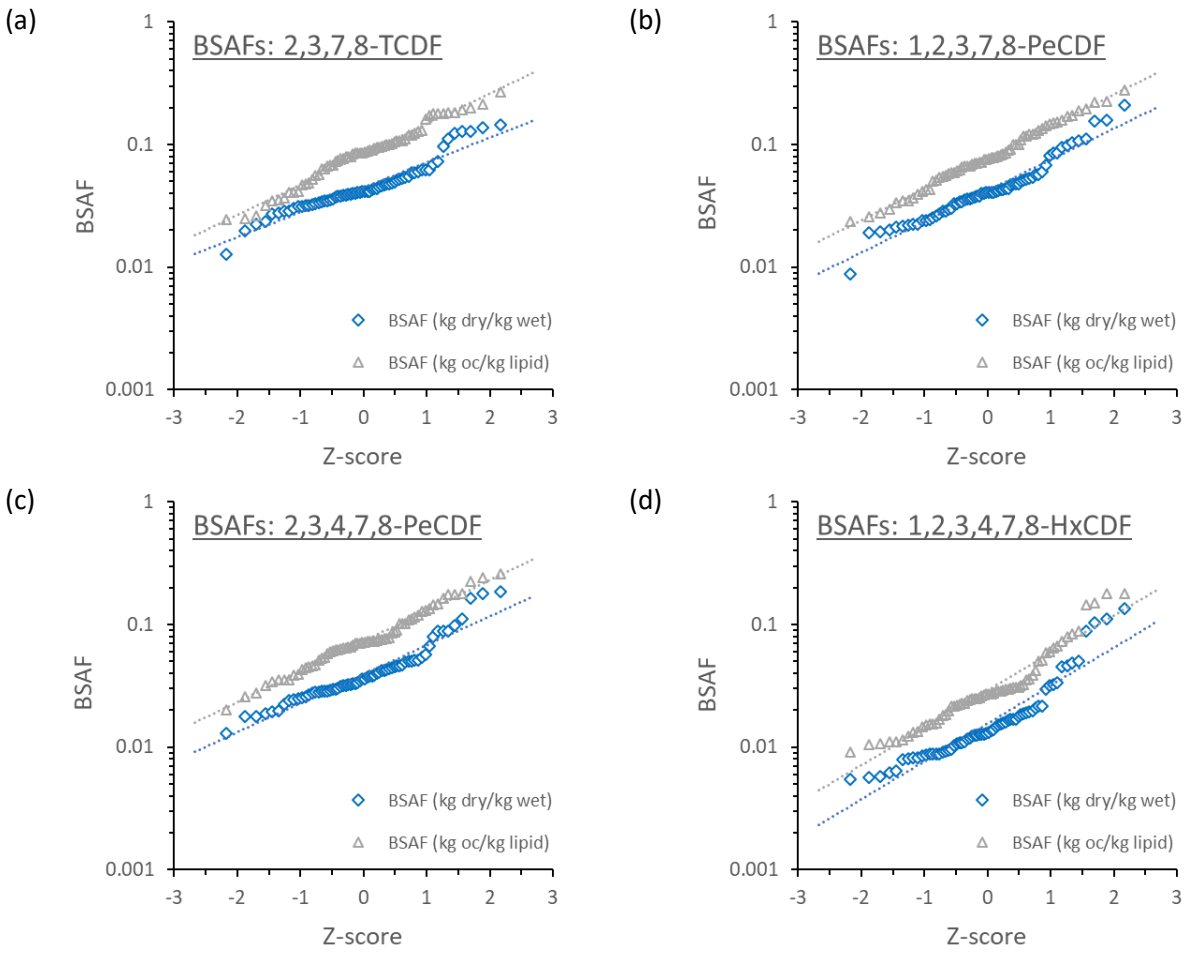

Figure A-3. Comparison of lipid:organic normalization of 28-day BSAF and non-normalized 28-day BSAF probability distributions for PCDF congeners.

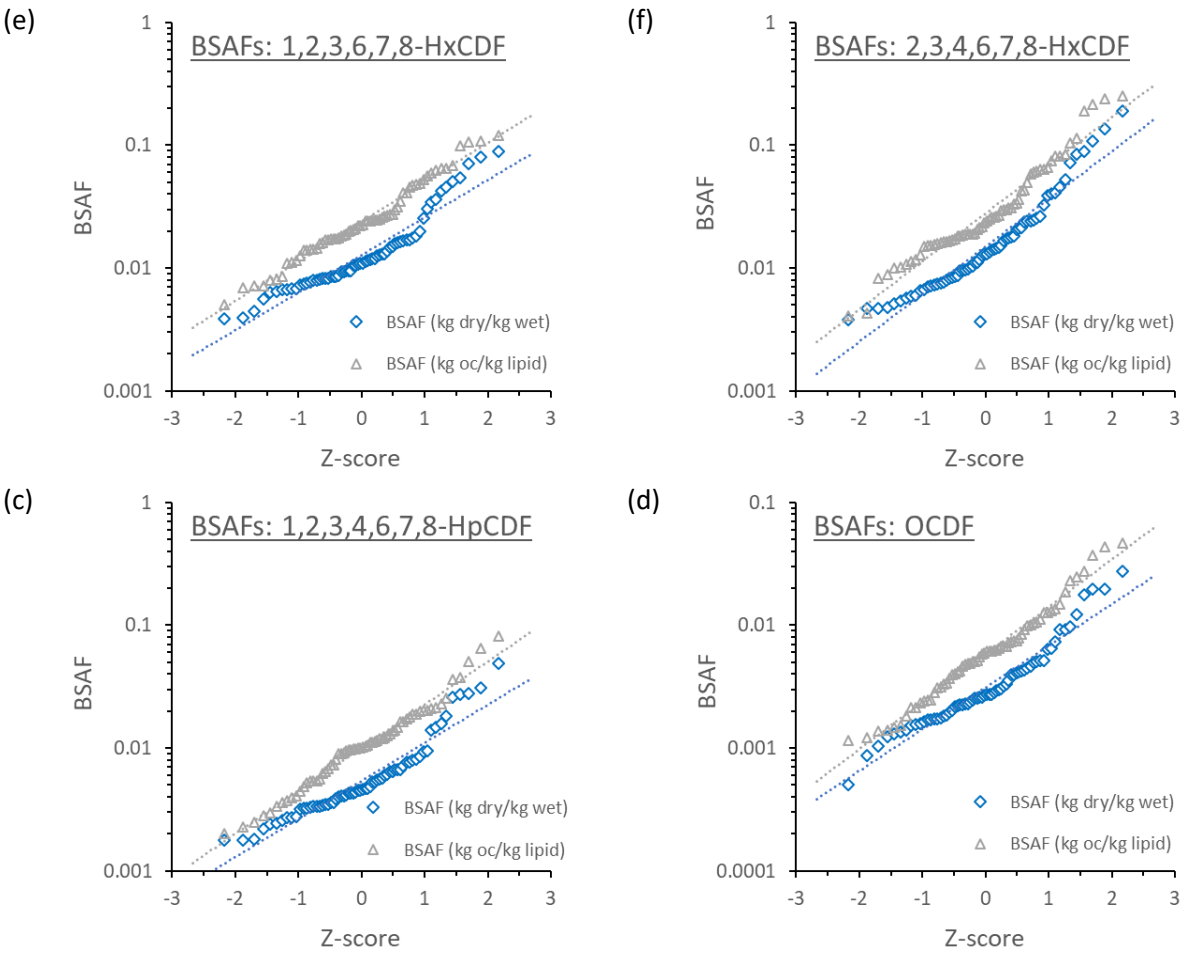

Figure A-3 (continued). Comparison of lipid:organic normalization of 28-day BSAF and non-normalized 28-day BSAF probability distributions for PCDF congeners. Note: there is a change in scale on the y-axis for OCDF.

NY/NJ Harbor Contamination Assessment and Reduction Project

CARP II

Task 5: Develop a method (or model) for predicting bioaccumulation of sedimentary contaminants in dredged material test organisms

Appendix B. Data extraction from Microsoft Access CARP II database

July 2023

Data extraction from CARP II Microsoft Access CARP II database

CARP II bioaccumulation data were organized and extracted from the CARP II database as follows:

1. tblChems in the CARP II database was expanded to include additional information on PCB and PCDD/F congeners. The expanded table was named "tblChems(kjf_7_2022)." This included molecular weight, log K_{ow}, ΔH_{ow}, and Setschenow constants that are listed in Tables A-2 and A-3). In addition, dihedral angles, and number of chlorines in the ortho, meta and para positions was added for PCB congeners. Cross-listed Information of co-eluting PCB congeners was also expanded to include final adjustments of co-eluting congeners that were made to account for overlapping co-elutes in the sediment/tissue dataset (SGS AXYS) and porewater dataset (University of Rhode Island) (see Table A-4). Finally, information on potential metabolizable sites on the PCB congeners and other physico-chemical parameters for PCBs and PCDD/Fs that were extracted from the UFZ-LSER database were also include in "tblChems(kjf_7_2022)" but were not used in the final bioaccumulation analyses.
2. A series of Microsoft Access queries were developed to reformat information on PCB homologs, PCB congeners, PCDD/F congeners and ancillary data into a form that could be readily extracted and used in Microsoft Excel data analyses. Flow diagrams for data extraction of PCB homologs, PCB congeners and PCDD/F congeners are presented in Figures B-1 through B-3. Final datsheet views from the "kjf_2022-09-11_PCB_homolog_Combined _Query", "kjf_2022-09-11_PCB_homolog_Combined _Query" and "kjf_2022-09-11_PCB_homolog_Combined _Query" were copied into separate Excel worksheets for further data analyses.

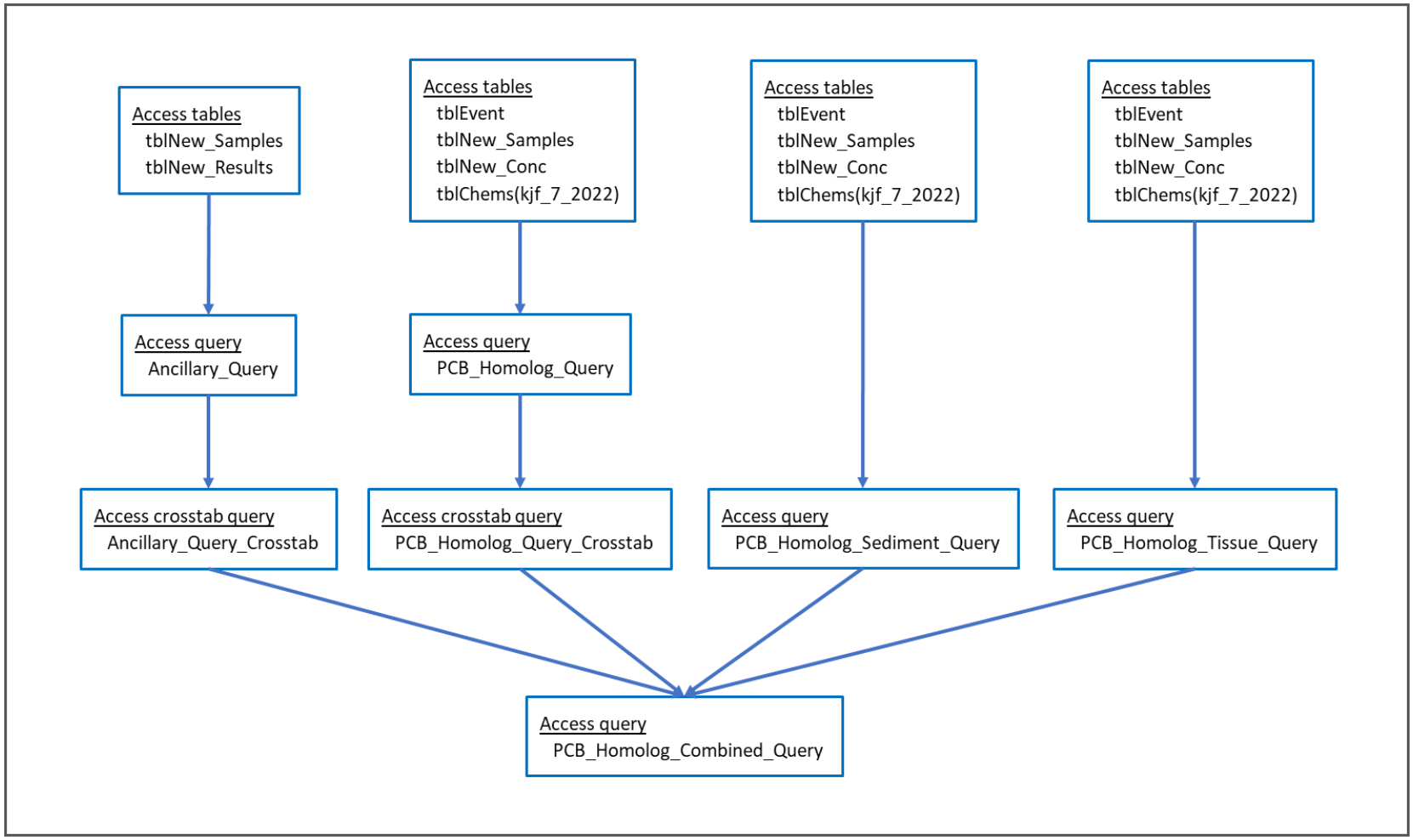

Figure B-1. Flow diagram for organizing and extracting PCB homolog data for the Microsoft Access CARP II database. Final datasheet views from the "kjf_2022-09-11_PCB_Homolog_Combined _Query" were copied into a separate Excel worksheet for further data analyses. Note: names for all of the Access queries and crosstab queries began with "kjf_2022-09-11…".

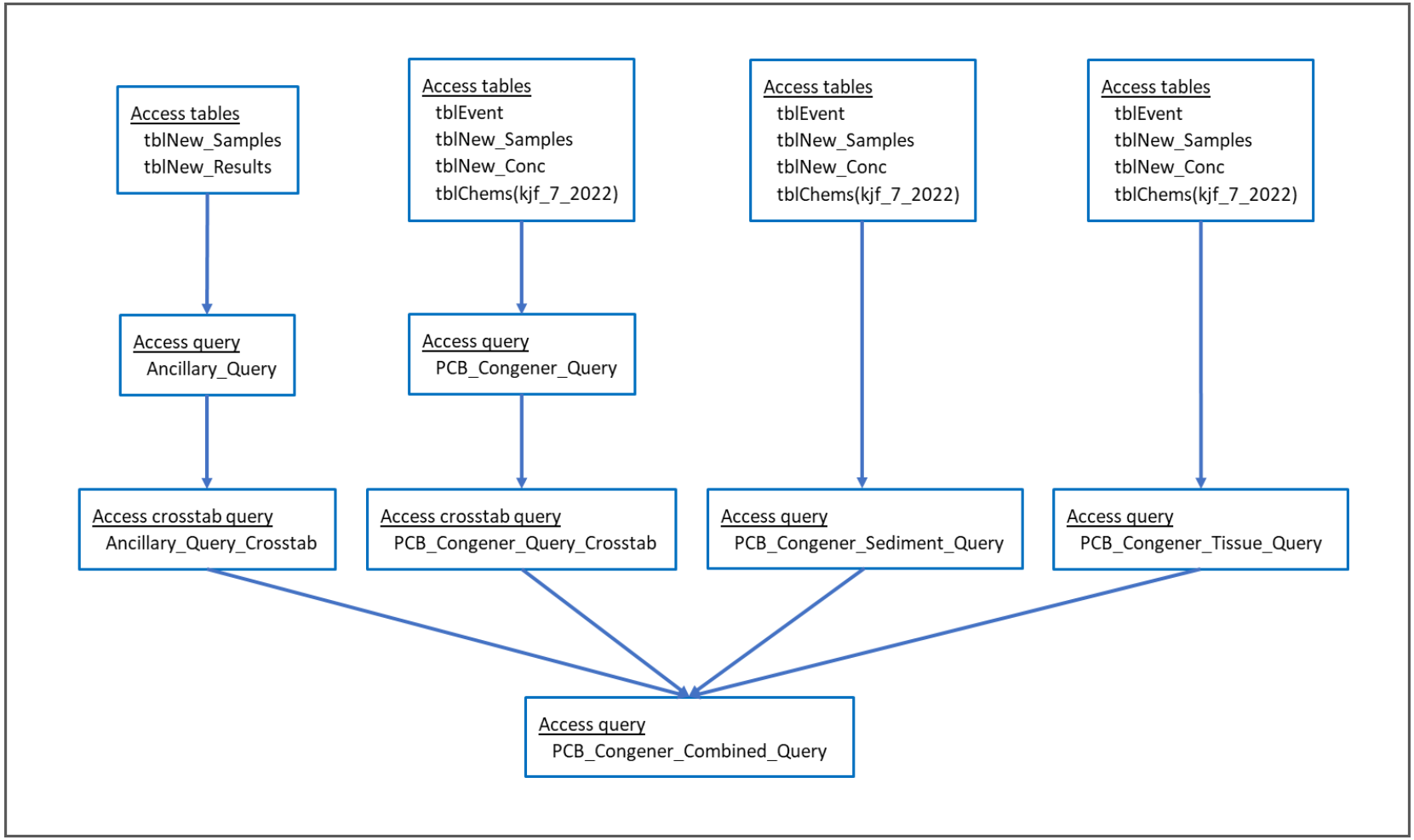

Figure B-2. Flow diagram for organizing and extracting PCB congener data for the Microsoft Access CARP II database. Final datasheet views from the "kjf_2022-09-11_PCB_Congener_Combined _Query" were copied into a separate Excel worksheet for further data analyses. Note: names for all of the Access queries and crosstab queries began with "kjf_2022-09-11…".

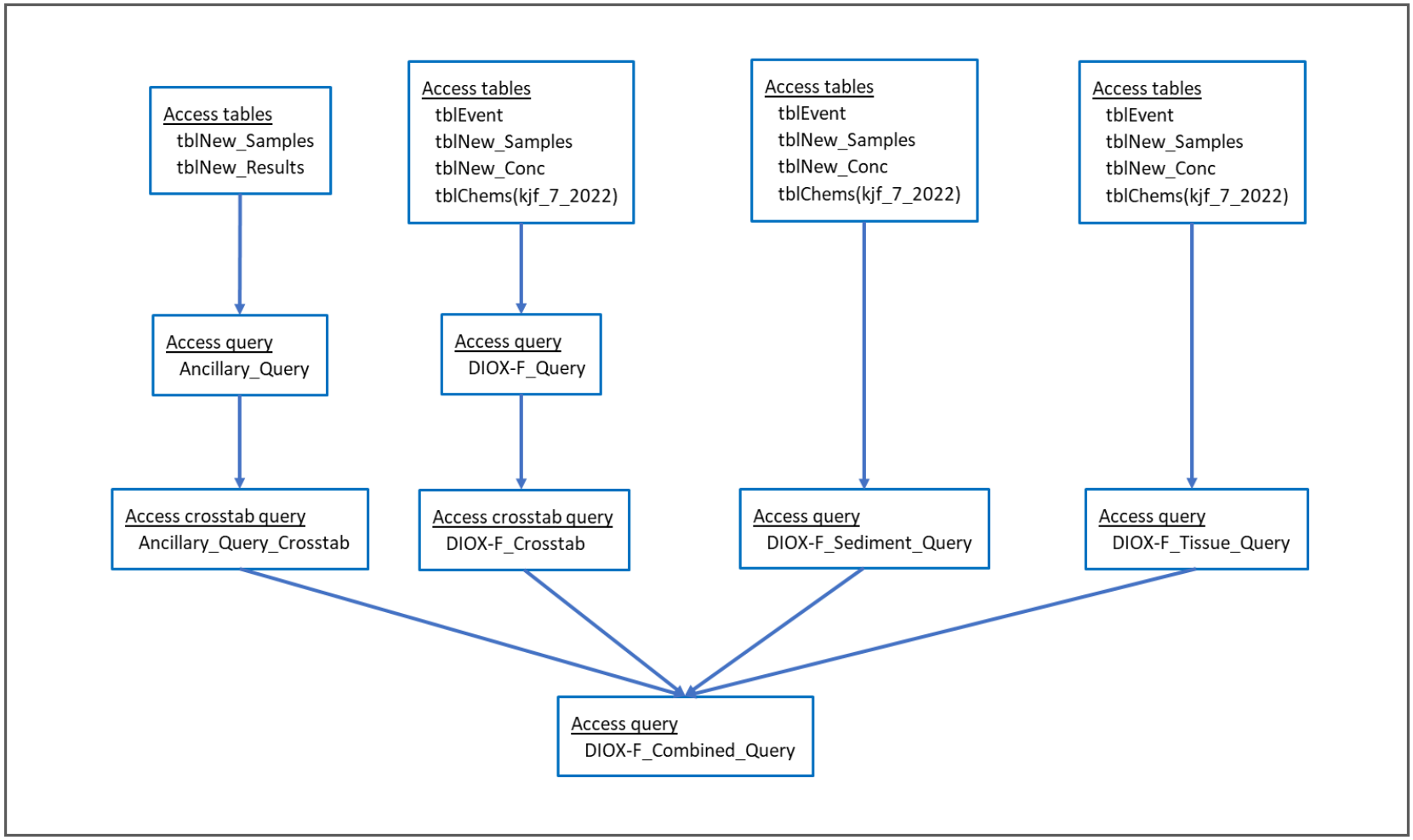

Figure B-3. Flow diagram for organizing and extracting PCDD/F congener data for the Microsoft Access CARP II database. Final datasheet views from the "kjf_2022-09-11_DIOX-F_Combined _Query" were copied into a separate Excel worksheet for further data analyses. Note: names for all of the Access queries and crosstab queries began with "kjf_2022-09-11…".

NY/NJ Harbor Contamination Assessment and Reduction Project

CARP II

Task 5: Develop a method (or model) for predicting bioaccumulation of sedimentary contaminants in dredged material test organisms

Appendix C. Poster presentation for the two-box bioaccumulation model

from

da Luz N, Farley KJ. "Effect of Black Carbon and Organism Growth Rates on Bioaccumulation of PCBs in Benthic Invertebrates: A Modeling Perspective." Poster Presentation, Battelle Ninth International Conference on Remediation of Contaminated Sediments, New Orleans LA, 9-12 January 2017.

July 2023

Effect of Black Carbon and Organism Growth Rates on Bioaccumulation of PCBs in Benthic Invertebrates: A Modeling Perspective

Nelson da Luz, Kevin J. Farley Ph.D.

Department of Civil and Environmental Engineering, Manhattan College

Introduction

Laboratory testing with benthic invertebrates have often been used in to assess bioaccumulation-mediated risks at contaminated sediment sites. In these evaluations, laboratory results have typically been presented in terms of Biota Sediment Accumulation Factors (BSAFs) to relate organism body burdens to contaminant concentrations in sediment.

$$BSAF_{lipid,oc} = \frac{y_{lipid}}{f_{TOC}}$$

Large variations in BSAFs however have been reported for laboratory bioaccumulation test results. For example, see BSAFs for field-collected worms in NY-NJ Harbor below. Bioavailability of contaminants in sediments (e.g., as affected by the presence of black carbon) has been cited as a possible reason for these large variations. In addition to bioavailability, other factors such as the nutritional content of the sediment organic carbon, organism bioenergetics and feeding behavior are expected to play an important role. The objective of this work was to develop and apply a "two-box" mechanistic-based model to evaluate the effect of black carbon and organism bioenergetics on the bioaccumulation of PCBs in benthic invertebrates.

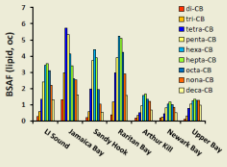

Acknowledgments

This project has been funded through the Blasland, Bouck and Lee Endowment at Manhattan College.

References

1. Contamination Assessment and Reduction Project. A Model for the Evaluation and Management of Contaminants of Concern in Water, Sediment, and Biota in the NY/NJ Harbor Estuary. 2007.
2. Burkhard, L. P., Mount, D. R., Highland, T. L., Hockett, J. R., Norberg-King, T., Billa, N., Hawthorne, S. B., Miller, D. J. and Grabarski, C. B. (2013), Evaluation of PCB bioaccumulation by *Lumbriculus variegatus* in field-collected sediments. Environmental Toxicology and Chemistry, 32: 1495–1503.
3. Nielsen, A.M., Eriksen, N.T., Iversen, J.J.L., and Riisgård, H.U. (1995). Feeding, growth and respiration in the polychaetes Nereis diversicolor (facultative filter-feeder) and N. virens (omnivorous) - a comparative study. Mar. Ecol. Prog. Ser. 125: 149-158.
4. Werner, D., Hale, S.E., Ghosh, U. and Luthy, R.G., (2009). Polychlorinated biphenyl sorption and availability in field-contaminated sediments†. Environmental science & technology, 44(8), pp.2809-2815.

2-Box Bioaccumulation Model

The model includes uptake and back-diffusion across the respiratory membrane; ingestion and egestion of digestible organic carbon (oc), non-digestible organic carbon (ndoc) and black carbon (BC); chemical transfer across the gut wall; and organism growth.

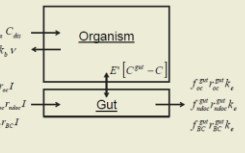

Organism: Dry weight basis

$$\frac{dv}{dt} = k_e C_{diz} - k_g v + E'\left[C^{pw} - C\right] - k_z v$$

Gut: Assume the gut rapidly reaches steady state

$$0 = E'\left[C - C^{pw}\right] + \left[f_{oc} r_{oc} + f_{ndoc} r_{ndoc} + f_{BC} r_{BC}\right] \cdot I - \left[f_{oc}^{pw} r_{oc}^{pw} + f_{ndoc}^{pw} r_{ndoc}^{pw} + f_{BC}^{pw} r_{BC}^{pw}\right] k_e$$

Solution: For 28-day accumulation

$$v = \frac{k_e C_{diz} + \alpha\left[f_{oc} r_{oc} + f_{ndoc} r_{ndoc} + f_{BC} r_{BC}\right]}{k_{ssz}} \cdot \left[1 - e^{-k_{ssz} \cdot 28\,days}\right]$$

$$k_{ssz} = k_g + \alpha\gamma \frac{K_{oc}}{K_{lipid}} \frac{f_{ox}}{f_{lipid}} + k_z$$

$$\alpha = \frac{E'}{\gamma K_{ow} + E'} \; ; \; \gamma = \left[f_{oc}^{pw} r_{oc}^{pw} + f_{ndoc}^{pw} r_{ndoc}^{pw} + f_{BC}^{pw} r_{BC}^{pw}\right] k_e$$

Proof of Concept: NY-NJH

Model parameters that were specified for initial model runs for New York/New Jersey Harbor (NY-NJH) are given below. Two approaches were considered in fitting NY-NJH field data.

1. No BC at the outer harbor site
2. Zero growth at inner harbor site due to a larger fraction of non-digestible organic carbon. (Note: log K_{BC} was set equal to 6.5 for these model run to better describe observed BSAFs, particularly at the outer harbor site.)

Model Parameters

f_{TOC}	0.07	$l = k_e$	50% / day
f_{lipd}	0.01	k_g	6% / day
f_{BC}	0.007	R_{basal}	1% / day
f_{ox}	0.125	α_{growth}	0.2
$C(O_2)$	1 mg/L	assim	1.0
E'	150 L/g_{ow}-day		
R	$R = R_{basal} + \alpha_{growth} \lvert k_g \rvert$		Ref. 3
f_{oc}	$f_{oc} = \left(R + k_g\right) \frac{0.4}{1 \cdot assim}$		
f_{ndoc}	$f_{ndoc} = f_{TOC} - f_{oc}$		
K_{oc}	$K_{oc} = K_{ow}$		
K_{lipd}	$K_{lipd} = K_{ow}$		
K_{BC}	$\log K_{BC} = 0.91 \log K_{ow} + 1.37$ or $\log K_{BC} = 6.5$		Ref. 4

1. Effect of Black Carbon

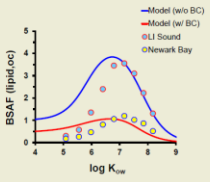

2. Effect of Organism Growth Rate

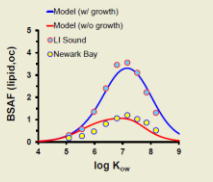

Application: GR and UHR

The 2-box bioaccumulation model was run using bioaccumulation data for *Lumbriculus variegatus* in fresh water systems for Grasse River (GR) and Upper Hudson River (HR) sediments (Burkhard et al 2013). The model was run using site-specific values for f_{TOC}, f_{BC} and k_g. Organism ingestion / egestion rates were back-calculated using the site-specific growth rates and assuming that 90% of the total organic carbon was digestible organic carbon.

For positive organism growth rates, the model provides a reasonably description of PCB accumulation using the constant log K_{BC} of 6.5. However, the model could not describe PCB accumulation in cases with negative growth rates.

GR-44: f_{TOC} = 0.045, f_{BC} = 0.0032, k_g = 0.5% / day

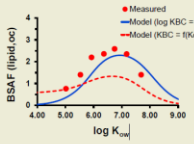

HR-88: f_{TOC} = 0.013, f_{BC} = 0.0034, k_g = 0.42% / day

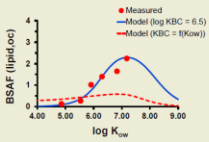

HR-92: f_{TOC} = 0.04, f_{BC} = 0.017, k_g = -1.1% / day